Optimizing Generation Expansion Planning With Operational Uncertainty: A Multistage Adaptive Robust Approach

Adam Abdin, Aakil Caunhye, Enrico Zio, Michel-Alexandre Cardin

Optimizing Generation Expansion Planning With Operational Uncertainty: A Multistage Adaptive Robust Approach

Adam F. Abdin[a,*], Aakil Caunhye[b], Enrico Zio[c,d], Michel-Alexandre Cardin[e]

[a]*Laboratoire Genie Industriel, CentraleSupélec, Université Paris-Saclay*
3 Rue Joliot Curie, 91190 Gif-sur-Yvette, France
[b]*University of Edinburgh Business School, Edinburgh, United Kingdom*
[c]*Mines ParisTech, PSL Research University, CRC, Sophia Antipolis, France*
[d]*Department of Energy, Politecnico di Milano, Italy*
[e]*Dyson School of Design Engineering, Imperial College London, United Kingdom*

Abstract

This paper presents a multistage adaptive robust generation expansion planning model, which accounts for short-term unit commitment and ramping constraints, considers multi-period and multi-regional planning, and maintains the integer representation of generation units. The uncertainty of electricity demand and renewable power generation is taken into account through bounded intervals, with parameters that permit control over the level of conservatism of the solution. The multistage robust optimization model allows the sequential representation of uncertainty realization as they are revealed over time. It also guarantees the *non-anticipativity* of future uncertainty realizations at the time of decision-making, which is the case in practical real-world applications, as opposed to two-stage robust and stochastic models. To render the resulting multistage robust problem tractable, decision rules are employed to cast the uncertainty-based model into an equivalent mixed integer linear (MILP) problem. The re-formulated MILP problem, while tractable, is computationally prohibitive even for moderately sized systems. We, thus, propose a solution method relying on the reduction of the information basis of the decision rules employed in the model, and validate its adequacy to efficiently solve the problem. The importance of considering

*Corresponding author
Email address: adam.abdin@centralesupelec.fr (Adam F. Abdin)

multistage robust frameworks for accounting for net-load uncertainties in generation expansion planning is illustrated, particularly under a high share of renewable energy penetration. A number of renewable penetration scenarios and uncertainty levels are considered for a case study covering future generation expansion planning in Europe. The results confirm the effectiveness of the proposed approach in coping with multifold operational uncertainties and for deriving adequate generation investment decisions. Moreover, the quality of the solutions obtained and the computational performance of the proposed solution method is shown to be suitable for practical policy-making generation expansion planning problems, seeking to evaluate the impact of uncertainty on future system-wide performance.

Keywords:

Multistage adaptive robust optimization, Uncertainty treatment, Generation Expansion Planning, Unit commitment, High renewable energy systems

---

Acronyms:

CCGT	Combined Cycle Gas Turbine
CF	Capacity Factor
CMIP5	Coupled Model Intercomparison Project phase 5
DRO	Distributionally Robust Optimization
GEP	Generation Expansion Planning
HVAC	High Voltage Alternating Current
HVDC	High Voltage Direct Current
IGEP-UC	Integrated Generation Expansion Planning and Unit Commitment
IRES	Intermittent Renewable Energy Sources
LHS	Left Hand Side
LNS	Load Not Served
MILP	Mixed Integer Linear Programming
MS-AARC	Multistage Affinely Adjustable Robust Counterpart
MS-RC	Multistage Robust Counterpart
PV	Photo-Voltaic
RCP	Representative Concentration Pathway
RHS	Right Hand Side
RO	Robust Optimization
SO	Stochastic Optimization
UC	Unit Commitment
UR	Uncertainty Range
WCD	Worst-Case Deterministic

1. Introduction

The planning of power systems expansions to accommodate intermittent renewable energy sources (IRES), such as wind and solar power, has received extensive attention in recent years (Pereira et al., 2017; Dagoumas and Koltsaklis, 2019). The challenges brought by the variability of IRES production emphasize the need to account for operational flexibility as an integral part of power systems planning models (Alizadeh et al.,

2016). Operational flexibility is a time-and-state specific attribute of the power system that most notably relates to its short-term ramping abilities to adequately respond to changes in net-load. This net-load variation is significantly increasing in modern power systems because of changing user patterns driven by smart-devices (Li et al., 2018a), the increase of renewable energy production (Neetzow, 2021) and the expected prevalence of electric vehicles with vehicle-to-grid capabilities (Gunkel et al., 2020), among others.

Long-term generation expansion planning (GEP) in an environmentally conscious way remains one of the most challenging and critical problems facing system planners. In the literature, different modeling frameworks have been proposed to hedge for the shortages in operational flexibility in future power systems expansion, among which, a new class of integrated generation expansion planning (GEP) and unit commitment (UC) models (IGEP-UC) (Palmintier and Webster, 2011). As opposed to the prior prevalent modeling simplification of averaging the short-term operational conditions within long-term planning models, these integrated models combine long-term investment decisions and short-term hourly operational decisions within a single optimization framework. This way, ramping requirements characterizing the system flexibility are explicitly accounted for. Examples of these models can be found in: (Koltsaklis and Georgiadis, 2015) in which a multi-regional IGEP-UC model is presented with features that allow the evaluation of different policy targets, (Pereira et al., 2017) which consider a similar integrated IGEP-UC planning model and investigate a number of planning scenarios with high level of IRES integration, and (Abdin and Zio, 2018) in which a comprehensive assessment framework with adequate metrics is proposed to optimize the IGEP-UC problem with high IRES penetration. However, because each of the GEP and UC models is itself large and computationally intensive, particularly if realistic integer decisions such as investment and commitment of generation units are to be maintained, most of the literature integrating both models within a single optimization have been limited to deterministic instances.

Accounting for the uncertainty in IRES supply and in system load, however, is a

significant concern for ensuring adequate system operation. Uncertainties in power systems can be classified into short-term and long-term uncertainties (Zhang and Conejo, 2017). Long-term uncertainties include investment costs, policy incentive schemes and fuel prices. Short-term uncertainties are more concerned with operational parameters such as hourly load variations, hourly renewable resource availability as well as transmission lines and generation system failures, among others. Power systems are increasingly facing both supply and demand uncertainties in addition to the inter-temporal intermittency of renewable production. If these uncertainties are not taken into account when planning power system expansion, severe consequences may occur. Two examples clearly stand out in modern power systems: the first is the large amount of load shedding that occurred in Texas in 2008 due to the unexpected drop in wind power generation (National Renewable Energy Laboratory U.S. and United States. Department of Energy. Office of Scientific and Technical Information, 2008) and, the second is the more recent blackout caused by the cold-spell in the ERCOT-Texas power system (Smead, 2021).

Two popular approaches have been often applied to address the supply and demand uncertainties in power systems. The first is stochastic optimization (SO), which models the uncertain parameters by means of scenarios generated from pre-defined probability distributions and solve for an expected value over the uncertainty realizations. SO models have been widely employed to handle uncertainties both for the GEP problem (Koltsaklis and Nazos, 2017; Park and Baldick, 2015) and for the UC problem (Quan et al., 2015; Wang et al., 2013; Shi and Oren, 2018), separately. However, one of the important limitation of the SO approach is that it assumes that the probability distribution of the uncertain parameters are known or can be estimated with high accuracy, which is not always the case, particularly within long term-planning models.

The other popular approach for handling uncertainty is Robust Optimization (RO), which models uncertain parameters by means of distribution-free bounded intervals. RO methods typically attempt to ensure protection against worst-case uncertainty realizations, as opposed to expected ones. In addition, when considering RO with

adjustable decisions, usually formulated as two-stage or multistage models with recourse, the model can be reformulated as a convex optimization problem and handled efficiently.

Because of these characteristics, RO methods have been widely used in the power systems literature. However, most of the research has focused on proposing models to treat uncertainty-driven power system expansion or short-term uncertain operational problems, separately. (Chen et al., 2019) proposes a two-stage RO planning and operation method for Energy Hub design, considering precise energy storage models. In (Caunhye and Cardin, 2018), a two-stage adaptive RO model is proposed for long-term generation and transmission expansion under supply uncertainties but with no explicit consideration of short-term system performance. (Moret et al., 2020) develops and uses an RO energy planning model to investigate the risk of over-capacity in power systems investment. More recently, research has started to explore the use of a modeling paradigm closely related to RO, called distributionally robust optimization (DRO). DRO seeks to overcome one of the important criticism for RO methods which is the over-conservatism of the solutions obtained by incorporating partial knowledge about the probability distribution of the uncertain parameters, when available. In power system planning, this approach has been also used to address the transmission expansion planning problem (Guevara et al., 2020). On the other hand, explicit short-term operational uncertainties have been considered in robust unit commitment models, such as in (Zhou et al., 2019; Ye and Li, 2016; Bertsimas et al., 2013; Lorca et al., 2016; Lorca and Sun, 2017), as well as robust power system flexibility assessment methods (Zhao et al., 2015, 2014), but without considering the power systems expansion planning. Short-term operational constraints were, however, considered in (Li et al., 2018b) for power system planning but only through an aggregation of the time-steps that does not consider the hourly chronological evolution of the system.

Research work that considers the integrated long-term expansion planning and short-term operational optimization under uncertainty is much less explored in the literature. Among the recent research work that treats this problem is the work of

(Verastegui et al., 2019), which proposes an RO power system planning model with short-term dispatch constraints. However, in their work they only consider a two-stage robust model and do not consider the integer nature of the investment and unit commitment decisions. Other work, such as (Zhang and Conejo, 2017), propose a robust model for transmission expansion planning combining short-term and long-term uncertainties using a three-level optimization approach, and (Velloso et al., 2020) presents a DRO approach, also for the transmission expansion planning, considering both long-term and short-term uncertainties in the system; yet, both papers do not consider the generation expansion problem.

Despite recent progress, some important gaps remain in the literature treating GEP under uncertainty. Most notably, to the best of our knowledge, no research work has considered a *multistage* robust treatment for the integrated IGEP-UC problem. Multistage robust models were developed in the work of (Dehghan et al., 2018) which only deals with transmission and not generation expansion planning, in (Liu et al., 2018) which considers a multistage *stochastic* generation expansion with no consideration for UC constraints, and in (Lorca et al., 2016) in which only the short-term UC model is treated but without the generation expansion.

The distinction between two-stage and multistage robust models is important and is, sometimes, not clearly understood. Multistage models are *non-anticipative* in that the uncertainty realization is revealed sequentially and the decision-maker (the optimization model) cannot anticipate future uncertainty realizations for taking current decisions. Two-stage models assume a look-ahead into the whole uncertainty realizations to adjust decisions at each time step, which does not reflect how decisions are taken in practice. Clearly, this leads to a different model formulation and outcome. Indeed, for the short-term unit commitment problem, (Lorca et al., 2016) has demonstrated how two-stage robust models, as a modeling framework, may lead to infeasibility in the dispatch problem when the generation ramping capability is actually limited. This motivates the major relevance of this work in addressing the IGEP-UC planning problem within a multistage robust optimization setting, where uncertainty

realizations are non-anticipative and are revealed sequentially, as is especially the case for planning systems with a high share of IRES penetration.

Finally, while recognizing that many studies treating uncertain power systems planning problems work with stochastic programming techniques, for the multistage case treated in this paper stochastic programming would require time-evolving probability distributions, which significantly adds to the problem complexity. Multistage stochastic programs are, to our current knowledge, computationally intractable, even when medium-level accuracy is required, and Monte-Carlo sampling is used for scenario generation. Shapiro and Nemirovski (2005) show how the computational efforts to solve multistage stochastic programming with sample average approximation increase exponentially when the number of stages grow. In our case, we have the same number of stages as the shortest-time period throughout the time horizon. This makes it problematic to conceive the problem in a multistage stochastic programming setting.

To address these challenges, this paper proposes a multistage, multi-period and multi-regional robust IGEP-UC model to help policymakers make decisions about future generation investments informed by IRES and system load uncertainty considerations[1]. The model integrates long-term integral GEP decisions with short-term unit commitment constraints and linearized optimal power dispatch in the power network.

We develop a tractable form of the multistage robust model and propose a novel solution method relying on the reduction of the information basis of the decision rules employed. The information basis reduction method proposed in our work is different than other approaches that have been proposed in the literature (see for example (Lorca et al., 2016) and (Ben-Tal et al., 2004)) since the information about the values of the

[1]The type of centralized planning model considered in this paper may not necessarily give the same results as a game-theory market-based planning model, where each company decides on its own investment decisions in a competitive environment. However, centralized planning models are widely used by policymakers and regulators to identify a system-wide optimal investment strategy, and thus, ensure that the market outcome does not deviate significantly from this optimal strategy by setting proper policy incentives.

uncertainty realizations and the decision variables at the *most recent* time step is always maintained to inform the decisions in the subsequent time-step. This is a unique feature to our solution approach that, to best of our knowledge, has not been explored in the robust power systems planning literature. Other computational reduction methods proposed relies on different information reduction concepts including the reduction of spatial information or of temporal information without maintaining information about the most recent state of the system. We show that, for our integrated power system planning problem, our proposed approach leads to close to optimal solutions with a significant reduction in computational time.

We validate the performance of the proposed model and solution method on a case-study based on the European power system spanning 8 European countries. We highlight a number of insights regarding the uncertainty impact on IGEP-UP models, notably related to the investment decisions, generation mix, renewable energy integration and shedding, and transmission lines utilization and congestion, among others. The proposed model and solution framework are shown to be relevant for practical decision-making in planning highly uncertain, future power systems.

In summary, the main contributions of this work are:

- The paper proposes a multi-period, multi-regional and multistage adaptive robust optimization model for the long-term integrated generation expansion planning and unit commitment (IGEP-UC) problem to explicitly accommodate net-load uncertainties due to a significant shares of renewable energy production. To the best of the authors knowledge, this is the first treatment of the integrated (IGEP-UC) problem within a multistage adjustable robust optimization setting. Moreover, unlike other models that similarly treat long-term planning and short-term operation under uncertainty in a single optimization, our model maintains firm integer representation of both investment and unit commitment decisions.

- Within the presented multistage adaptive robust model, we propose a novel description of the uncertainty set combining the uncertainty describing the system

load and renewable energy capacity factors within a *single* set. This reduces the burden for the decision maker of estimating the conservativeness level of each source of uncertainty separately.

- To resolve the computational complexity of the fully adaptive multistage model, we propose a novel solution method by introducing a new parameter which controls the level of information considered within the decision rules implemented in the model. We fully investigate the outcome given by the solution method proposed and show that significant computational gains can be achieved while maintaining the significance of the results within, at most, a 1% optimality tolerance.

- Moreover, the results obtained by the proposed solution method empirically suggest the Markovian nature of the IGEP-UC model where only information about the most recent state of the system is sufficient to fully inform the decisions in the following time-step. While this observation may need to be further investigated, it could have significant practical implications in understanding and treating similar models.

2. Deterministic IGEP-UC model

The full formulation of the deterministic IGEP-UC model can be found in Appendix A. Briefly, the multi-period integrated IGEP-UC model proposed seeks to minimize the total discounted system costs over the planning horizon. These costs include: the annualized investment costs in conventional and renewable generation units (A.1a), yearly operational and maintenance costs (A.1b) and variable operational costs of the power system, such as start-up costs for conventional generation units (A.1c), production costs and cost of load-not-served (lns) (A.1d). The investment decisions are subject to long-term constraints including the budget limit, adequacy requirement, renewable penetration level, and short-term constraints including supply-demand balance, generation limits, unit commitment decisions, ramping limits and minimum up

and down times. The model is formulated as a mixed integer linear program (MILP) considering annual long-term generation expansion planning constraints and hourly short-term unit commitment decisions.

The proposed formulation explicitly considers discrete generation units investment and commitment decisions, and employs the integer clustering method to allow a tractable optimization of large-sized systems with a high number of generation units (Palmintier and Webster, 2014). Typically, many decision variables, such as the investment, start-up and shut-down decisions, are binary variables calculated for each generation unit. The integer clustering method groups the decisions for similar and/or identical units in a single integer variable represented by a technology cluster. In this approach, each generation unit is still represented individually for each decision variable, but handled collectively within the cluster. To achieve this, for the mathematical formulation, each generation technology is represented by a cluster identifier. Discrete variables in the problem can, then, take any positive integer value to account for individual generation units, i.e.: $\boldsymbol{q}, \boldsymbol{x}, \boldsymbol{u}, \boldsymbol{z}, \boldsymbol{v} \in \mathbb{Z}_0^+$. Other modeling adjustments necessary to properly use the integer clustering methods are directly employed in the proposed formulation. A full discussion about this approach can be found in (Palmintier and Webster, 2014).

3. Robust IGEP-UC model formulation

Generation expansion planning and operation is subjected to significant uncertainties, particularly, with regards to the short-term power demand and availability of renewable resources. The accumulation of errors in considering these uncertainties for long-term planning can lead to significant errors in investment decisions. Specific policy targets such as the desired levels of renewable production in the system and the desired levels of carbon reduction could be failed to be reached. In particular, the uncertainties in the ramping capabilities of the system can only be considered if the unit commitment problem is properly integrated within the long-term generation expansion planning. To ensure investment plans that are robust to these uncertainties,

this section develops a robust counter-part of the proposed model which is adequate for practical usage by decision makers and capable of properly capturing the most salient features of the short-term uncertainties in the system.

3.1. Definition of the uncertainty set

The robust IGEP-UC model considers a distribution-free characterization of both the electricity demand and the IRES supply uncertainties in each location and at each hour of the planning horizon. Those uncertainties, in addition to posing a significant challenge for the hourly dispatch decisions of thermal and nuclear units, also implicitly result in uncertainties in ramping requirements, start-up and shut-down decisions from one time-period to the next. To characterize these uncertainties, the hourly load vector, $\boldsymbol{L}$, takes on a range of possible values bounded by a lower ($\underline{\boldsymbol{L}}$) and upper ($\bar{\boldsymbol{L}}$) bounds. Similarly, the capacity factor $\boldsymbol{CF}$, which models IRES supply uncertainty, varies in the range $[\underline{\boldsymbol{CF}}, \bar{\boldsymbol{CF}}]$. Different from the commonly employed separate definition of uncertainty sets for each source of uncertainty, in this work, a *unique* polyhedral uncertainty characterization that combines both IRES supply and load demand uncertainties is proposed. For this formulation of the uncertainty set, the decision maker has to estimate a single level of conservatism for both uncertainty sources, which reduces the burden of estimating the conservativness level for each source of uncertainty separately. We reasonably assume that under a high share of IRES penetration, the decision maker primarily cares about the worst-case uncertainty realization in which the highest system load and lowest IRES availability occur simultaneously, to adequately plan and operate the remaining thermal and nuclear units in the system. The uncertainty set is, then, defined for the worst case *net-load* realization (highest load ($\bar{\boldsymbol{L}}$) - lowest IRES-CF ($\underline{\boldsymbol{CF}}$). The uncertainty set is, therefore, formulated as:

$$\mathcal{U}_i^{yst}(\Gamma) = \Bigg\{ \beta_i^{yst} \in \mathbb{R}_+, CF_{ig}^{yst} \in \mathbb{R}^{|G^{(res)}|} :$$

$$\underline{\beta}_i^{yst} \leq \beta_i^{yst} \leq \bar{\beta}_i^{yst}, \quad \underline{CF}_{ig}^{yst} \leq CF_{ig}^{yst} \leq \bar{CF}_{ig}^{yst}, \forall g \in G^{(res)},$$

$$\beta_i^{yst} - \sum_{g \in G^{(res)}} CF_{ig}^{yst} \leq \Gamma_i \cdot (\bar{\beta}_i^{yst} - \sum_{g \in G^{(res)}} \underline{C}F_{ig}^{yst}) \Bigg\}, \forall i \in I, y \in Y, s \in S, t \in T \quad (1)$$

Where, $\boldsymbol{\beta}$ represents the normalized load time-series such as $\left(\boldsymbol{\beta} = \boldsymbol{L}/L^{Max}\right)$, and L^{Max} is the maximum load value of the load time-series. This is done to ensure the numerical consistency for the calculation of the uncertainty set in which both the normalized load time-series vector ($\boldsymbol{\beta}$) and IRES-CF vector ($\boldsymbol{CF}$) vary in the same range. For this formulation, $\boldsymbol{\beta}$ varies in the range $\left[\underline{\boldsymbol{\beta}}, \bar{\boldsymbol{\beta}}\right]$.

Γ (≤ 1), represents the level of conservatism of the decision maker. In this setting, $\Gamma = 1$ signify that the load and IRES-CF can take on their full range of possible values. For $\Gamma < 1$, the uncertainty set excludes the absolute worst-case situations, which is where all sub-period loads are at their highest values and all IRES-CF are at their lowest values. The lower bound of the uncertainty budget Γ can be derived through the observation that: $\underline{\beta}_i^{yst} - \sum_{g \in G^{(res)}} \bar{CF}_{ig}^{yst} \leq \beta_i^{yst} - \sum_{g \in G^{(res)}} CF_{ig}^{yst} \leq \Gamma_i \cdot (\bar{\beta}_i^{yst} - \sum_{g \in G^{(res)}} \underline{C}F_{ig}^{yst}), \forall i \in I, y \in Y, s \in S, t \in T$ This implies that: $\underline{\beta}_i^{yst} - \sum_{g \in G^{(res)}} \bar{CF}_{ig}^{yst} \leq \Gamma_i \cdot (\bar{\beta}_i^{yst} - \sum_{g \in G^{(res)}} \underline{\mathrm{CF}}_{ig}^{yst})$, $\forall i \in I, y \in Y, s \in S, t \in T$. Hence, $\Gamma_i \geq \dfrac{\underline{\beta}_i^{yst} - \sum_{g \in G^{(res)}} \bar{CF}_{ig}^{yst}}{\bar{\beta}_i^{yst} - \sum_{g \in G^{(res)}} \underline{\mathrm{CF}}_{ig}^{yst}}$, $\forall i \in I, y \in Y, s \in S, t \in T$, from which we can calculate the lower bound of Γ_i as: $\Gamma_i \geq \max\limits_{y,s,t} \left\{ \dfrac{\underline{\beta}_i^{yst} - \sum_{g \in G^{(res)}} \bar{CF}_{ig}^{yst}}{\bar{\beta}_i^{yst} - \sum_{g \in G^{(res)}} \underline{C}F_{ig}^{yst}} \right\}, \forall i \in I.$

3.2. Robust Model Formulation

The planning problem under uncertainty is formulated as a multistage adaptive robust optimization model, where uncertainties are revealed sequentially over time, and the decision maker cannot anticipate the uncertainty realization before their occurrence. In this model, investment and unit commitment decisions are here-and-now decisions required to be robust to uncertainty realizations and the optimal power dispatch decisions are *wait-and-see* decisions required to be subject to (and thus, flexible to) uncertainty realizations. The objective of the uncertainty-driven robust model is to minimize the total cost of the investment decisions plus the worst-case cost of the recourse dispatch decisions while ensuring full immunization of the investment plans

and their operational schedules over all possible uncertainty realizations. To formulate the uncertainty-driven robust model, we let $\mathcal{V}^{yst}(=\{\boldsymbol{\beta}^{yst}, \boldsymbol{CF}^{yst}\})$ to denote the uncertainty realizations from the first time-period up to the current time-period t, respecting the non-anticipativity assumption. Given that recourse decisions $\big(p_{ig}^{yst}(\mathcal{V}^{yst})$, $lns_i^{yst}(\mathcal{V}^{yst})$, $f_{ij}^{yst}(\mathcal{V}^{yst})$ and $\theta_i^{yst}(\mathcal{V}^{yst})\big)$ made in a time period t are adaptable on the full history of uncertainty realization from the first time period up to t, the formulation of the multistage robust counterpart (MS-RC) of problem the IGEP-UC problem (A.1a)-(A.3k) is:

Objective function

$$\min_{\boldsymbol{\Omega},\boldsymbol{\Theta}(\cdot)} \Bigg\{ \text{(A.1a)-(A.1b)} + \sum_{y\in Y}\sum_{s\in S}\sum_{t\in T} \max_{\mathcal{V}^{yst}\in\, \mathcal{U}^{yst}} \sum_{i\in I} \Bigg[\sum_{g\in G} \left(\frac{Marg\_C_g^y}{(1+DF)^y} \cdot p_{ig}^{yst}(\mathcal{V}^{yst}) \right) + \frac{Lns\_C}{(1+DF)^y} \cdot lns_i^{yst}(\mathcal{V}^{yst}) \Bigg] \Bigg\} \tag{2a}$$

subject to:

investment and commitment constraints

$$\text{constraints (A.2a)-(A.2g)} \tag{2b}$$

full immunization against uncertainty constraint

$$\text{s.t.} \quad \forall \mathcal{V}^{yst} \in \mathcal{U}^{yst}, \left(\mathcal{U}^{yst} \triangleq \prod_{\substack{i\in I \\ t'\in[t]}} \mathcal{U}_i^{yst'}, [t] \triangleq \{1,...,t\} \right),$$

$$\exists p_{ig}^{yst}(\cdot), lns_i^{yst}(\cdot), f_{ij}^{yst}(\cdot), \theta_i^{yst}(\cdot) \in \mathbb{R}_+, \quad \forall i,j \in I, g \in G, y \in Y, s \in S, t \in T \tag{2c}$$

dispatch constraints *(multistage recourse decisions)*

$$\sum_{g\in G} p_{ig}^{yst}(\mathcal{V}^{yst}) + lns^{yst}(\mathcal{V}^{yst}) - \sum_{j\in N_{(i)}^+} f_{ij}^{yst}(\mathcal{V}^{yst}) + \sum_{j\in N_{(i)}^-} f_{ji}^{yst}(\mathcal{V}^{yst}) - \beta_i^{yst} \cdot L^{Max} = 0, \quad \forall i \in I, y \in Y, s \in S, t \in T \tag{2d}$$

$$\sum_{s\in S}\sum_{t\in T}\sum_{g\in G^{(res)}} p_{ig}^{yst}(\mathcal{V}^{yst}) \geq Res^{(lvl)} \cdot \sum_{s\in S}\sum_{t\in T} \bar{\beta}_i^{yst} \cdot L^{Max}, \forall i \in I^c, y \in Y \tag{2e}$$

$$p_{ig}^{yst}(\mathcal{V}^{yst}) \leq u_{ig}^{yst} \cdot \bar{P}_g, \quad \forall i \in I, g \in G^{(th)}, \forall y \in Y, s \in S, t \in T \tag{2f}$$

$$p_{ig}^{yst}(\mathcal{V}^{yst}) \geq u_{ig}^{yst} \cdot \underline{P}_g, \quad \forall i \in I, g \in G^{(th)}, \forall y \in Y, s \in S, t \in T \tag{2g}$$

$$p_{ig}^{yst}(\mathcal{V}^{yst}) - p_{ig}^{yst-1}(\mathcal{V}^{yst-1}) \leq u_{ig}^{yst-1} \cdot \bar{UR}_g + z_{ig}^{yst} \cdot St\_P_g, \forall i \in I, \\ g \in G^{(th)}, y \in Y, s \in S, t \in T \setminus \{1\} \tag{2h}$$

$$p_{ig}^{yst-1}(\mathcal{V}^{yst-1}) - p_{ig}^{yst}(\mathcal{V}^{yst}) \leq u_{ig}^{yst-1} \cdot \bar{DR}_g, \forall i \in I, g \in G^{(th)}, \\ y \in Y, s \in S, t \in T \setminus \{1\} \tag{2i}$$

$$p_{ig}^{yst}(\mathcal{V}^{yst}) \leq x_{ig}^{y} \cdot \bar{P}_g \cdot CF_{ig}^{yst}, \quad \forall i \in I, g \in G^{(res)}, \forall y \in Y, s \in S, t \in T \tag{2j}$$

$$-2\bar{\theta} \leq \theta_i^{yst}(\mathcal{V}^{yst}) - \theta_j^{yst}(\mathcal{V}^{yst}) - \mathcal{X}_{ij} \cdot f_{ij}^{yst}(\mathcal{V}^{yst}) \leq 2\bar{\theta}, \\ \forall (i,j) \in \mathcal{F}, y \in Y, s \in S, t \in T \tag{2k}$$

$$-\bar{f}_{ij} \leq f_{ij}^{yst}(\mathcal{V}^{yst}) \leq \bar{f}_{ij}, \quad \forall (i,j) \in \mathcal{F}, y \in Y, s \in S, t \in T \tag{2l}$$

$$-\bar{\theta} \leq \theta_i^{yst}(\mathcal{V}^{yst}) \leq \bar{\theta}, \quad \forall i \in I, y \in Y, s \in S, t \in T \tag{2m}$$

$$\theta_i^{yst}(\mathcal{V}^{yst}) = 0, \quad \forall i \in I^{ref}, y \in Y, s \in S, t \in T \tag{2n}$$

3.3. Multistage affinely adjustable robust counterpart of the IGEP-UC problem

Notice that the multistage objective definition of (2a) (not to be confused with the *multiperiod* aspect of the problem) is the compact form of the equivalent nested *"min-max-min"* formulation, for each time period within the uncertainty set (Lorca et al., 2016):

$$\min_{\mathbf{\Omega} \in X} \left\{ c^\top \Omega + \max_{\boldsymbol{\mathcal{V}}^1 \in \boldsymbol{\mathcal{U}}^1} \min_{\mathbf{\Theta}^1 \in \Psi_1(\mathbf{\Omega}, \boldsymbol{\mathcal{V}}^1, \mathbf{\Theta}^0)} \left\{ \mathbf{c}^\top \mathbf{\Theta}^1 + \ldots + \max_{\boldsymbol{\mathcal{V}}^T \in \boldsymbol{\mathcal{U}}^T} \min_{\mathbf{\Theta}^T \in \Psi_T(\mathbf{\Omega}, \boldsymbol{\mathcal{V}}^T, \mathbf{\Theta}^{T-1})} \mathbf{c}^\top \mathbf{\Theta}^T \right\} \right\} \tag{3}$$

where $\Psi_t(\mathbf{\Omega}, \boldsymbol{\mathcal{V}}^t, \mathbf{\Theta}^{t-1}) \triangleq \{\mathbf{\Theta}^t : \text{ (A.3a)-(A.3k) are satisfied}\}$.

This definition separates the uncertainty set over each time period. Because of the full immunization constraint (2c) and the fact that the uncertain parameters are real-valued, the robust counterpart is semi-infinite. Linear decision rules are conventionally implemented to make the problem tractable (Kuhn et al., 2011). Applying this method, which results in a multistage affinely adjustable robust counterpart (MS-AARC), is appealing in that it results in an MILP model that can be solved using available solvers and conventional Bender's type decomposition methods, and does not require

significant tailor-made development of solution methods. In this paper, the MS-AARC of the proposed model is obtained by replacing the vector of recourse variables using the following linear relationship:

$$\boldsymbol{\Theta}^{yst}(\mathcal{V}^{yst}) = \boldsymbol{\Theta_0}^{yst} + \sum_{i' \in I} \sum_{t' \in [t]} \boldsymbol{\Theta_l}_{i'}^{ystt'} \cdot \beta_{i'}^{yst'} + \sum_{g' \in G^{(res)}} \sum_{i' \in I} \sum_{t' \in [t]} \boldsymbol{\Theta_c}_{i'g'}^{ystt'} \cdot CF_{i'g'}^{yst'} \quad (4)$$

where $[t] \triangleq \{1, ..., t\}$ and $\left(\boldsymbol{\Theta_0}^{yst}, \boldsymbol{\Theta_l}_{i'}^{ystt'}, \boldsymbol{\Theta_c}_{i'g'}^{ystt'}\right)$ are the coefficients of the linear decision rule. Then, in the resulting model, the constraints can be processed into a finite number of linear constraints, relying on a duality-based reformulation to obtain the final MILP problem. An illustration of how the processing is achieved for one equality and one inequality constraints under our proposed definition for the uncertainty set is given below.

Equality constraint: Consider the supply-demand equality constraint (A.3a). Replacing the uncertainty dependent variables $p_g^{yst}(\mathcal{V}^{yst})$ and $lns^{yst}(\mathcal{V}^{yst})$ following equation (4), and re-arranging the terms, we obtain:

$$\begin{aligned}
&\left(\sum_{g \in G} p0_{ig}^{yst} + lns0_i^{yst} - \sum_{j \in N_{(i)}^+} f0_{ij}^{yst} + \sum_{j \in N_{(i)}^-} f0_{ji}^{yst}\right) + \\
&\sum_{i' \in I, i' \neq i} \sum_{t' \in [t-1]} \left(\sum_{g \in G} pl_{ii'g}^{ystt'} + lnsl_{ii'}^{ystt'} - \sum_{j \in N_{(i)}^+} fl_{ii'j}^{ystt'} + \sum_{j \in N_{(i)}^-} fl_{jii'}^{ystt'}\right) \cdot \beta_{ii'}^{yst'} + \\
&\left(\sum_{g \in G} pl_{iig}^{ystt} + lnsl_{ii}^{ystt} - \sum_{j \in N_{(i)}^+} fl_{iij}^{ystt} + \sum_{j \in N_{(i)}^-} fl_{jii}^{ystt} - L^{Max}\right) \cdot \beta_{ii}^{yst} + \\
&\sum_{i' \in I} \sum_{t' \in [t]} \sum_{g' \in G^{(res)}} \left(\sum_{g \in G} pC_{ii'gg'}^{ystt'} + lnsc_{ii'g'}^{ystt'} - \sum_{j \in N_{(i)}^+} fc_{ii'jg'}^{ystt'} + \sum_{j \in N_{(i)}^-} fc_{jii'g'}^{ystt'}\right) \cdot CF_{ii'g'}^{yst'} = 0,
\end{aligned}$$

$$\forall (i,j) \in \mathcal{F}, y \in Y, s \in S, t \in T \quad (5a)$$

From this, we know that equality (5a) is valid *iff* equations (5b)-(5e) are satisfied:

$$\sum_{g \in G} p0_{ig}^{yst} + lns0_i^{yst} - \sum_{j \in N_{(i)}^+} f0_{ij}^{yst} + \sum_{j \in N_{(i)}^-} f0_{ji}^{yst} = 0, \forall (i,j) \in \mathcal{F}, y \in Y, s \in S, t \in T \quad (5b)$$

$$\sum_{g\in G} p_{l_{ii'g}}^{ystt'} + lns_{l_{ii'}}^{ystt'} - \sum_{j\in N_{(i)}^{+}} f_{l_{ii'j}}^{ystt'} + \sum_{j\in N_{(i)}^{-}} f_{l_{jii'}}^{ystt'} = 0, \quad \forall (i,j)\in\mathcal{F}, i'\in I, i'\neq i,$$

$$y\in Y, s\in S, t\in T, t'\in[t-1] \tag{5c}$$

$$\sum_{g\in G} p_{l_{ii'g}}^{ystt'} + lns_{l_{ii'}}^{ystt'} - \sum_{j\in N_{(i)}^{+}} f_{l_{ii'j}}^{ystt'} + \sum_{j\in N_{(i)}^{-}} f_{l_{jii'}}^{ystt'} = L^{Max}, \quad \forall (i,j)\in\mathcal{F}, i'\in I, i'=i,$$

$$y\in Y, s\in S, t\in T, t'=t \tag{5d}$$

$$\sum_{g\in G} p_{C_{ii'gg'}}^{ystt'} + lns_{c_{ii'g'}}^{ystt'} - \sum_{j\in N_{(i)}^{+}} f_{c_{ii'jg'}}^{ystt'} + \sum_{j\in N_{(i)}^{-}} f_{c_{jii'g'}}^{ystt'} = 0, \quad \forall (i,j)\in\mathcal{F}, i'\in I, g'\in G^{res},$$

$$y\in Y, s\in S, t\in T, t'\in[t-1] \tag{5e}$$

Inequality constraint: For the maximum generation production limit inequality (2f), the constraint, after applying the affine relationship (4), becomes:

$$p_{0_{ig}}^{yst} + \sum_{i'\in I}\sum_{t'\in[t]} p_{l_{ii'g}}^{ystt'}\cdot L_{i'}^{yst'} + \sum_{i'\in I}\sum_{t'\in[t]}\sum_{g'\in G^{(res)}} p_{c_{ii'gg'}}^{ystt'}\cdot CF_{i'g'}^{yst'} \leq \bar{P}_g\cdot u_{ig}^{yst},$$

$$\forall i\in I, g\in G^{(th)}, y\in Y, s\in S, t\in T \tag{6a}$$

Re-arranging the terms of the constraint, given that an uncertainty-affected constraint LHS $\leq$ RHS, where LHS contains all uncertainty terms and RHS contains the rest, is valid $\forall \mathcal{V}^{yst}\in\mathcal{U}^{yst}, t\in T$, *iff* $\max_{\mathcal{V}^{yst}\in\mathcal{U}^{yst}}$ LHS $\leq$ RHS, and applying this logic to inequality (6a), we get:

$$\max_{\mathcal{V}^{yst}\in\mathcal{U}^{yst}} \sum_{i'\in I}\sum_{t'\in[t]} p_{l_{ii'g}}^{ystt'}\cdot L_{i'}^{yst'} + \sum_{i'\in I}\sum_{t'\in[t]}\sum_{g'\in G^{(res)}} p_{c_{ii'gg'}}^{ystt'}\cdot CF_{i'g'}^{yst'} \leq \bar{P}_g\cdot u_{ig}^{yst} - p_{0_{ig}}^{yst},$$

$$\forall i\in I, g\in G^{(th)}, y\in Y, s\in S, t\in T \tag{6b}$$

Dualizing the left-hand side of the constraint by referring to the definition of the uncertainty set (1), and because of strong duality, this set of non-linear inequalities can be replaced by the set of linear inequalities (7a)-(7d), where $\boldsymbol{\pi}$ is the vector of dual variables associated with the bounds of the uncertainty set (1), such as:

$$\underline{\beta}_i^{yst} \leq \beta_i^{yst} : \boldsymbol{\pi_A} \tag{6c}$$

$$-\bar{\beta}_i^{yst} \leq \beta_i^{yst} : \boldsymbol{\pi_B} \tag{6d}$$

$$\underline{CF}_{ig}^{yst} \leq CF_{ig}^{yst} : \boldsymbol{\pi_C} \tag{6e}$$

$$-\bar{CF}_{ig}^{yst} \leq CF_{ig}^{yst} : \boldsymbol{\pi_D} \tag{6f}$$

$$\beta_i^{yst} - \sum_{g \in G^{(res)}} CF_{ig}^{yst} \leq \Gamma_i \cdot (\bar{\beta}_i^{yst} - \sum_{g \in G^{(res)}} \underline{CF}_{ig}^{yst}) : \boldsymbol{\pi_E} \tag{6g}$$

The dual linear equalities, thus, are formulated as:

$$\sum_{i' \in I} \sum_{t' \in [t]} (\pi_{A}{}_{ii'g}^{ystt'} \cdot \bar{\beta}_{i'}^{yst'} - \pi_{B}{}_{ii'g}^{ystt'} \cdot \underline{\beta}_{i'}^{yst'}) + \sum_{i' \in I} \sum_{t' \in [t]} \sum_{g' \in G^{(res)}} (\pi_{C}{}_{ii'gg'}^{ystt'} \cdot \bar{CF}_{i'g'}^{yst'} - \pi_{D}{}_{ii'gg'}^{ystt'} \cdot \underline{CF}_{i'g'}^{yst'})$$
$$+ \sum_{i' \in I} \sum_{t' \in [t]} \pi_{E}{}_{ii'g}^{yst} \cdot \Gamma_i \cdot (\bar{\beta}_{i'}^{yst'} - \sum_{g' \in G^{(res)}} \underline{CF}_{i'g'}^{yst'}) \leq \bar{P}_g \cdot u_{ig}^{yst} - p0_{ig}^{yst},$$

$$\forall i \in I, g \in G^{(th)}, y \in Y, s \in S, t \in T \tag{7a}$$

$$\pi_{A}{}_{ii'g}^{ystt'} - \pi_{B}{}_{ii'g}^{ystt'} + \pi_{E}{}_{ii'g}^{yst} \geq p_{l}{}_{ii'g}^{ystt'},$$

$$\forall i, i' \in I, g \in G^{(th)}, y \in Y, s \in S, t \in T, t' \in [t] \tag{7b}$$

$$\pi_{C}{}_{ii'gg'}^{ystt'} - \pi_{D}{}_{ii'gg'}^{ystt'} - \pi_{E}{}_{ii'g}^{yst} \geq p_{c}{}_{ii'gg'}^{ystt'},$$

$$\forall i, i' \in I, g \in G^{(th)}, g' \in G^{(res)}, y \in Y, s \in S, t \in T, t' \in [t] \tag{7c}$$

$$\pi_{A}{}_{ii'g}^{ystt'}, \pi_{B}{}_{ii'g}^{ystt'}, \pi_{C}{}_{ii'gg'}^{ystt'}, \pi_{D}{}_{ii'gg'}^{ystt'}, \pi_{E}{}_{ii'g}^{yst} \geq 0,$$

$$\forall i, i' \in I, g \in G^{(th)}, g' \in G^{(res)}, y \in Y, s \in S, t \in T, t' \in [t] \tag{7d}$$

Applying the same principle to all inequality and equality constraints, the semi-infinite robust counterpart is converted into a finite mixed-integer linear programming problem.

4. Solution method - Reduction of the information basis

As discussed in the previous section, in a multistage problem, recourse decisions made in a time period, t, depend on $\mathcal{V}^t\,(= \{\mathcal{V}^1, ..., \mathcal{V}^t\})$, i.e., the history of load and IRES-CF uncertainty realizations from the first time period up to t. In terms of model formulation, for each of the uncertainty realizations, an additional number of

dual variables and dual constraints are added to the MILP dual reformulation. The duality-based approach used to define the MS-AARC problem, therefore, can lead to an extremely large MILP problem that is not computationally feasible for practical-sized instances. In particular, for each set of constraints in the deterministic problem, the number of the respectively dualized MS-AARC additional variables and constraints are polynomially increasing in the number of time periods (T) and number of IRES units ($G^{(res)}$) considered.

The most important contributor to the above dimensionality issue in the MS-AARC is the increase of the number of variables and constraints by a triangular factor $\left(\frac{|T|\cdot(|T|+1)}{2}\right)$ of the number of periods considered. This factor arises because of the full dependency of the recourse variables on the entire history of realized uncertainty at every time period up to t. Following (Ben-Tal et al., 2004), we call this full affine dependency the "on-line information basis" since all historical information revealed about the uncertainties are taken into account to adapt the recourse decisions at the current time period.

We propose a solution method based on the reduction of the information basis for the decision rules, where only the most recent information about the uncertainty realizations are taken into account to adjust the recourse variables at the current time period. For this, a new parameter representing the information level, denoted h ($\leq |T|$), is introduced. This parameter represents the number of the most recent uncertainty realization to be taken into account in adjusting the recourse variable at the following time period. The full affine dependency is equivalent to setting $h = |T|$, whereas, if $h < |T|$, only the most recent uncertainty realizations are considered. In this case, the size of the equivalent MS-AARC set of constraints, the associated dual variables and the affine coefficient variables are reduced by an order of h^2, as shown in Table (1).

In the proposed information basis reduction method, the recourse decisions at each time step would implicitly maintain information on the full uncertainty realizations through the value attributed to the recourse actions at the most recent time step. In fact, the observations of the sensitivity analysis of the performance of the proposed

Table 1: Reduction factor of the number of variables and constraints via adjusting the information level "h"

	Reduction factor:
Dual Variables / Dual Constraints / Coefficient Variables	$\left(\frac{\lvert T\rvert - 1}{2} - h + \frac{h^2 + h}{2\lvert T\rvert}\right)$

solution method under different information levels, implies the Markovian nature of the IGEP-UC problem where only information on the most recent state of the system are sufficient to inform the decisions for the following state. In this way, the reduction method proposed is expected to simplify the problem structure (i.e. reduce the number of variables and constraints) with no impact on the quality of the solutions obtained. These propositions are confirmed by the analysis presented in the next sections.

To implement this information basis reduction method, the running index $[t]$ should be re-defined such as:

$$[t] \triangleq \begin{cases} \{1, ..., t\}, & \text{if } t \leq h \\ \{t - h, ..., t\}, & \text{if } t > h \end{cases} \tag{8}$$

The decision maker can, then, select the desired level of h to decide on the information level considered in the solution of the planning problem, if needed.

5. Validation of the proposed solution method on a multi-period single-region IGEP-UC problem

5.1. Power system description and implementation notes

We first consider a case study on a single-region multi-annual planning horizon covering 10 years from 2036 to 2045 for the validation of the solution method proposed. We consider the case of generation expansion planning in France, where the hourly system load is obtained through linear regression of the historical load time series of France for

the years 2006 to 2015 (publicly available at (RTE-France, 2017)), assuming a growth of 1.5% throughout the planning years. Wind and Solar-PV capacity factors are calculated from the wind speeds and solar irradiance data obtained from the Coupled Model Intercomparison Project phase 5 (CMIP5) climate experiments (Taylor et al., 2012), for the same time period, and for the geographical region of France. The grid level values obtained from the CMIP5 are, then, averaged for the whole geographical area of France. We consider wind and solar data from the Representative Concentration Pathways (RCP) 8.5 which assumes an increase in radiative forcing of +8.5 Wm^{-2}, compared to pre-industrial level. The dynamic operating conditions for the generation units are determined through representing each planning year by a number of uncertain representative days optimally obtained to allow the chronological representation of the system hourly state (Poncelet et al., 2017). The cost data for the power generation technologies are based on the IEA/NEA Projected Costs of Generating Electricity report (2015) (IEA/NEA, 2015). Table (2) summarizes the costs considered and the remaining technical characteristics of the power generation units.

Table 2: Technical and economic characteristics for the different generation technologies

Technology [i]	$\bar{P}_g$ [MW]	$\underline{P}_g$ [MW]	$U\bar{R}_g$ [MWh/min]	$D\bar{R}_g$ [MWh/min]	UM_g [hrs]	DM_g [hrs]	Inv_C_g [M€/MW]	$Marg\_C_g$ [€/MWh]	St_C_g [k€]
Nuclear	1400	700	$0.5\%\bar{P}$/min	$0.5\%\bar{P}$/min	12	48	3.95	9.33	15.0
Coal	1100	550	$1.5\%\bar{P}$/min	$1.5\%\bar{P}$/min	6	10	2.08	36.67	11.26
CCGT	550	165	$5\%\bar{P}$/min	$5\%\bar{P}$/min	3	5	1.02	69.00	7.53
On-Shore Wind	240	0	/	/	/	/	1.9	0	/
Solar-PV	180	0	/	/	/	/	1.5	0	/

For the uncertainty set, hourly load uncertainty is set to vary within 10% of the nominal values, while hourly IRES-CF uncertainty is set to vary within 20% around their nominal values. The MILP optimization models are coded in the Python programming language using the Pyomo software package (Hart et al., 2012) and solved on a PC with Intel Core i7 at 3.2GHz and 8GB memory using IBM ILOG-CPLEX with an optimality gap of 0.001%.

5.2. Worst-case analysis for robust power systems planning under net-load ramping uncertainty

In this section we illustrate the importance of considering a multistage robust problem compared to only solving the worst-case deterministic problem of the IGEP-UC, assuming a given uncertainty range. Indeed, it should be noted that according to the definition of the uncertainty set (1) and letting the uncertain parameters take on their full range of values ($\Gamma = 1$), the robust solution should be equivalent to the worst-case deterministic solution of the planning problem. This is because a worst-case solution that operationally satisfies all the highest hourly load occurrences ($\bar{\beta}$) and lowest IRES-CF ($\underline{CF}$) should be readily feasible to satisfy any combination of lower load and higher IRES-CF in the uncertainty range. We show that this is, indeed, the case if the time-coupling ramping constraints are ignored. However, enforcing the ramping constraints, in a multistage setting, implicitly re-defines the worst-case dispatch decisions in the IGEP-UC problem so that they are no longer defined by the worst load and IRES-CF, but also constrained to ensuring the ramping feasibility under all other uncertainty realizations of those parameters. This effect is not properly accounted for in non-causal operational models such as two-stage robust models or worst-case deterministic models, as has been shown in (Lorca et al., 2016). An example for this effect is the requirement to satisfy the system ramping needed in the case of the occurrence of the lowest IRES availability ($\underline{CF}_{t-1}$) at $t-1$ and the successive occurrence of the highest IRES availability ($\bar{CF}_t$) at t, if the uncertainties are to be realized in such a way. In this case, even a solution that is feasible to satisfy the net-load when the IRES availability are always at its lowest (worst-case uncertainty realization), might not be feasible in terms of ramping capacity available to meet all other combinations of IRES-CF realizations that are revealed sequentially. This is visually illustrated in Fig (1).

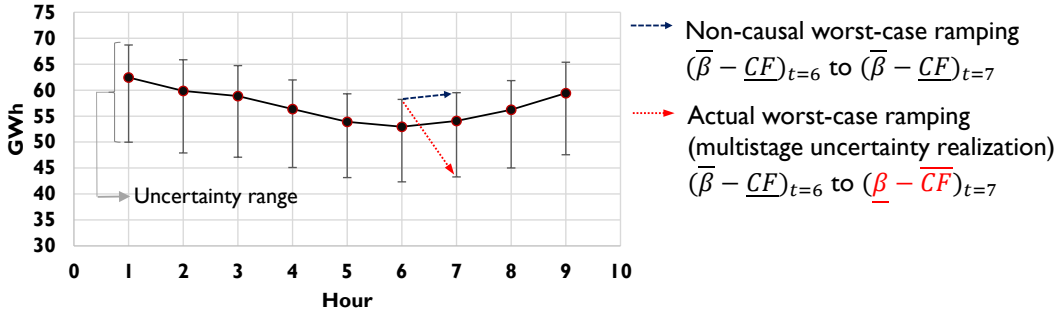

Figure 1: Illustration of non-causal worst-case ramping (e.g. as given by worst-case deterministic or two-stage robust models) and actual worst-case ramping (as sequentially revealed in a multistage temporal setting)

To evaluate this effect on the power system investment and operational decisions, the results of the case study are compared between the worst-case deterministic problem solution (denoted WCD) and the proposed MS-AARC planning model, for both the ramping-relaxed and ramping-enforced cases.

First, considering the ramping-relaxed case: as expected, both WCD and MS-AARC solutions are identical. The total objective value in both cases amounts to 112.38B€. The breakdown of the investment, operational and load not served (LNS) costs is shown in Fig. (2). On the other hand, by enforcing the ramping constraints, the solutions of both models are no longer identical. As shown in Fig. (2), the robust solution given by the MS-AARC model is +7.25% and +4.29% higher than the WCD solution, for the investment and operational costs, respectively.

In terms of investment decisions, Table (3) illustrates the total capacities installed per technology type for the cases considered. Similarly, it is shown that the new investments are the same for both WCD and MS-AARC solutions when ramping is ignored. Enforcing the ramping constraints leads to a shift in the installed capacities from the least flexible nuclear technology, to the most flexible CCGT technology. However, the ramping-enforced MS-AARC results confirm that neglecting the net-load uncertainties underestimates the actual flexible capacity needed for ensuring supply under the implicit worst case ramping realizations, revealed sequentially. This is shown as per the

investment results in an even lower nuclear capacity and higher CCGT ones.

The optimal WCD investment solution in these cases will, in fact, result in many infeasibilities for meeting the actual worst-case net-load ramping, as previously explained. The multistage decision making of the MS-AARC model accounts for those implicit worst-case rampings by adjusting the amount of flexible capacity installed, and how they are operated in terms of UC and dispatch decisions. This leads to a higher cost but more robust planning decisions.

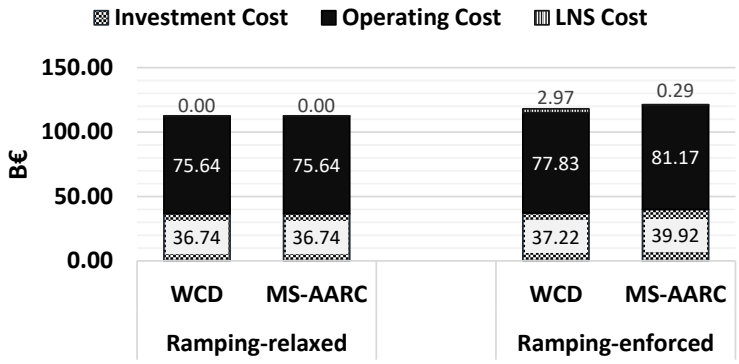

Figure 2: Breakdown of (annualized) investment, operational and LNS solution costs for the ramping-relaxed and ramping-enforced problems. Comparison between the WCD and MS-AARC solutions.

Table 3: Breakdown of total installed capacity per technology type for the ramping-relaxed and ramping-enforced problems. Comparison between the WCD and AARC solutions.

	Capacity Installed [GW]			
	Ramping-relaxed		Ramping-enforced	
Technology	WCD	MS-AARC	WCD	MS-AARC
Nuclear capacity	74.2	74.2	71.4	60.2
Coal capacity	11.0	11.0	18.7	19.8
CCGT capacity	14.3	14.3	8.8	13.2
Wind capacity	1.68	1.68	8.4	82.8
Solar capacity	85.32	85.32	90.54	10.44

Moreover, it is important to, also, quantify the performance of the MS-AARC model in terms of the amount of IRES shedding. This is because IRES shedding is

another means for managing inter-temporal ramping uncertainty. Notice in Table (4) the improved IRES shedding amounts as given by the MS-AARC (total of 1.46%) compared to WCD solution (total of 13.72%), when net-load ramping is accounted for.

Table 4: Breakdown of IRES shedding for the ramping-relaxed and ramping-enforced problems. Comparison between the WCD and MS-AARC solutions.

	Ramping-relaxed		Ramping-enforced	
	WCD	MS-AARC	WCD	MS-AARC
Wind power shedding	2.15%	2.15%	5.97%	1.51%
Solar power shedding	1.47%	1.47%	23.90%	0.07%
Total IRES shedding	1.49%	1.49%	13.72%	1.46%

5.3. Sensitivity of MS-AARC results to IRES penetration requirements and robustness levels

The previous section analyzed the importance of considering the uncertainties in net-load ramping within a multistage robust planning model. However, the results focused on the full robustness against uncertainty realization by setting the budget of uncertainty (Γ) to its maximum value. This part analyzes the solution of the proposed MS-AARC model for various levels of IRES penetration requirement (0%, 50% and 75%) and for various levels of conservativness level Γ (25%, 50% and 100%), to illustrate the relevance of the proposed approach for different planning contexts.

Table 5: Total number/capacity of generation units installed, per technology type, at the end of the planning horizon. Comparison between different levels of IRES penetration and of the budget of uncertainty Γ.

		Number of installed units					**Total capacity installed [in GW]**				
		Nuclear	Coal	CCGT	Wind	Solar	Nuclear	Coal	CCGT	Wind	Solar
0% IRES enforced	$\Gamma = 25\%$	40	14	15	69	0	56.0	15.4	8.25	16.56	0.00
	$\Gamma = 50\%$	41	15	16	117	0	57.4	16.5	8.8	28.08	0.00
	$\Gamma = 100\%$	43	17	24	253	14	60.2	18.7	13.2	60.72	2.52
50% IRES enforced	$\Gamma = 25\%$	35	8	29	308	0	49.0	8.8	15.95	73.92	0.00
	$\Gamma = 50\%$	36	10	29	300	30	50.4	11.0	15.95	72.00	5.40
	$\Gamma = 100\%$	42	12	33	342	45	58.8	13.2	18.15	82.08	8.10
75% IRES enforced	$\Gamma = 25\%$	31	10	26	420	585	43.4	11.0	14.3	100.80	105.30
	$\Gamma = 50\%$	32	11	28	453	601	44.8	12.1	15.4	108.72	108.18
	$\Gamma = 100\%$	38	11	34	516	712	53.2	12.1	18.7	123.84	128.16

The results summarized in Table (5) illustrate the total number of generation units installed, per technology type, at the end of the planning horizon and for each case considered. Table (5) also summarized the total capacity installed in GW (number of units * capacity of each unit). Notice, first, how the increased IRES penetration in the system has the global impact of shifting the investment decisions from nuclear generation to CCGT, under all budgets of uncertainty levels considered. Those units are characterized by better ramping capabilities, as per the assumptions used in the case study, and therefore, are deployed to ensure the adequacy of the system in response to the inter-temporal ramping uncertainties. Moreover, the results confirm that more of the flexible CCGT units are deployed as the robustness level of the system planning increases (i.e., higher Γ values) within each IRES scenario.

The temporal distribution of the planning decisions are shown in Fig (3) for the median IRES penetration case (IRES = 50%) and for $\Gamma = 25\%$ and $\Gamma = 100\%$, respectively. It is seen that, in all cases, the bulk of the investments are made in the first planning year. Notice that for the less conservative scenario (Fig. (3a), $\Gamma = 25\%$), there is an overall lower capacity investment and more distributed throughout the planning

horizon, compared to the more conservative case (Fig. (3c), $\Gamma = 100\%$). Particularly, more IRES capacity, both wind and solar, is commissioned in the early planning period of the latter case in response to the robustness requirement against higher CF uncertainty ranges.

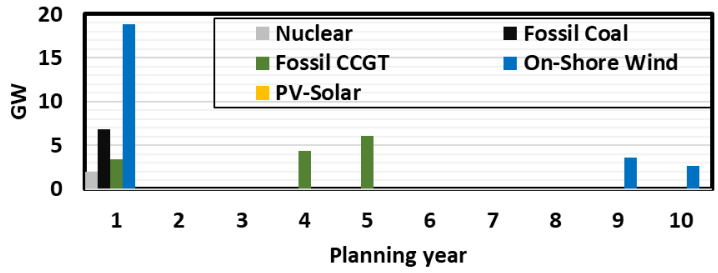

(a) $\Gamma = 25\%$

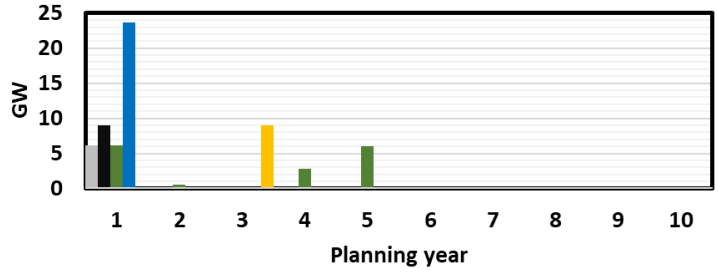

(b) $\Gamma = 50\%$

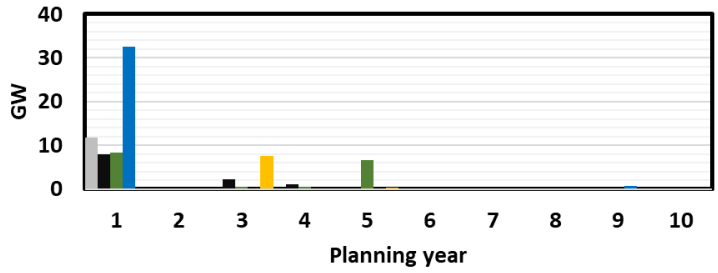

(c) $\Gamma = 100\%$

Figure 3: New capacity installed per technology type throughout the planning horizon for IRES penetration level = 50% and under different levels of Γ

5.4. Performance of the proposed solution method

The case studies presented in the previous sections were solved using the reduction of the information basis method proposed, setting the information level $h = 12$. Beyond this level, the problems is computationally challenging to be solved in practical

Table 6: Performance of the proposed solution method: comparison of the solutions obtained for different values of information level h parameter for the MS-AARC problem, compared to the fully affine dependent solution.

Information level (h)	1	2	3	4	5	6
Objective function difference	0.94%	0.95%	0.31%	0.50%	0.23%	0.05%
Information level (h)	7	8	9	10	11	12
Objective function difference	0.04%	0.49%	0.04%	0.48%	0.51%	0.26%
Information level (h)	13	14	15	16	17	18
Objective function difference	0.01%	0.03%	0.95%	0.48%	0.67%	0.61%
Information level (h)	19	20	21	22	23	24
Objective function difference	0.95%	0.50%	0.02%	0.97%	0.03%	0.03%

calculation time. To validate the choice for this information level and the effectiveness of the proposed solution method, we conduct a sensitivity analysis on the impact of varying the information level parameter h on the solution time and quality of the planning problem. The horizon considered for this purpose covers two planning years, each represented by 4 uncertain days of 24 hours. The parameter h, therefore, can vary from 1 to 24, representing the lowest to the highest historical information levels taken into account in the linear decision rules, respectively. The sensitivity is conducted by solving the resulting problems to an optimality gap of 1×10^{-7} for the highest possible accuracy for validation purposes. For each choice of the information level, the solution obtained is compared to the solution of the fully affine dependent problem (i.e. with no information reduction $h = 24$).

Table (6) shows the difference in the objective values obtained for solving the problem under different values of the information level parameter h, compared to the non-approximated problem. It is shown that in all cases, the objective function difference is at most 1%, with respect to the non-approximated solution.

With respect to the computational performance, Figure (4) shows that, indeed, the computational time significantly decreases as lower values of the historical information level h are considered. The solutions for the lowest h values is obtained within 10 to

40 seconds, and significantly increase as h increases. For the fully adjustable problem ($h = 24$), the solution time is 4375 seconds, compared to 11, 15 and 31 seconds for the three lowest h values considered.

It should be noted that the difference in the solution time across problems employing different information levels (h) is not strictly increasing as the problem size increase (higher values of h). As previously discussed, for each value of the information level h, a new MILP problem instance is created with a different number of variables and constraints. The resulting MILP problems are, then, solved using commercial solvers. The solution time for each instance depends on several factors, such as the speed of the initial heuristic in finding a good solution and the quality of the branching and cuts generated by the solver for each particular instance. This solution time does not necessarily correlate with the size of the problem instance, leading to a non-monotonous increase in computational time as larger problem instances are solved.

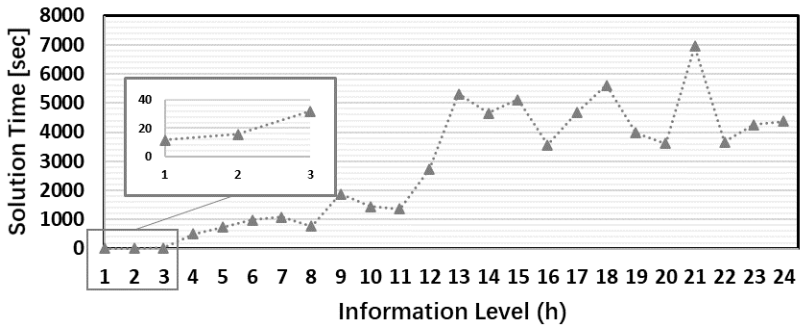

Figure 4: Impact of varying h on the computational time of the MS-AARC problem solution

The experimental results obtained for our case study confirm that the solutions obtained for different values of information level h, as per the proposed scheme, remain significantly representative of the solution of the fully affine dependent problem while gaining significant computational time. These results point out the Markovian nature of the MS-AARC model, i.e., that knowledge about the uncertainty realization for the most recent time step is sufficient to inform the decisions at the current time step, with no noticeable gains from considering older information about the uncertainty realiza-

tions (higher values of h) on the quality of the solution. The presented framework may, therefore, serve the decision maker to benchmark a wide range of practical planning scenarios under a robust approach, with a significant reduction in computational times.

6. Application to a multi-regional IGEP-UC planning problem with transmission constraints: European based case study

6.1. Extended case study with transmission network constraints

In this section, we illustrate a practical application for our proposed modeling and solution approach on an extended case study considering the transmission network and a multi-regional IGEP-UC planning problem. We consider a case study for the power system connecting neighboring mainland European countries, and in particular: Belgium, France, Switzerland, Luxembourg, the Netherlands, Germany, Italy and Spain. The data for the case study is obtained from the database of the model of the European electricity system at the transmission level, PyPSA-Eur, which is fully described in (Hörsch et al., 2018). Particularly, for the set of countries considered, data on network buses, transmission lines and their capacities are obtained from the database of PyPSA-Eur. The database of the PyPSA-Eur model contains all existing high-voltage alternating current (HVAC) and direct current (HVDC) lines in the European system. It also contains the lines planned by the European Network of Transmission System Operators for Electricity (ENTSO-E) in the Ten Year Network Development Plan (TYPNDP) (ENTSO-E, 2018). Moreover, hourly load data are obtain from the Open Power System Data project (OPSD, 2019) and calculated for each bus of each country based on the population and GDP data. We consider the historical hourly load data for the year 2019 and consider a projected 25% increase for these time series to project the demand for the year 2030. Conventional generation capacity existing at each bus is obtained from the powerplantmatching (PPM) database (Hofmann and Hörsch, 2019) and generation for wind and solar plants are based on data from the ERA5 reanalysis dataset (Hersbach et al., 2020). More information on the database

of PyPSA-Eur and the data gathering methods can be found in (Hörsch et al., 2018; Frysztacki et al., 2021).

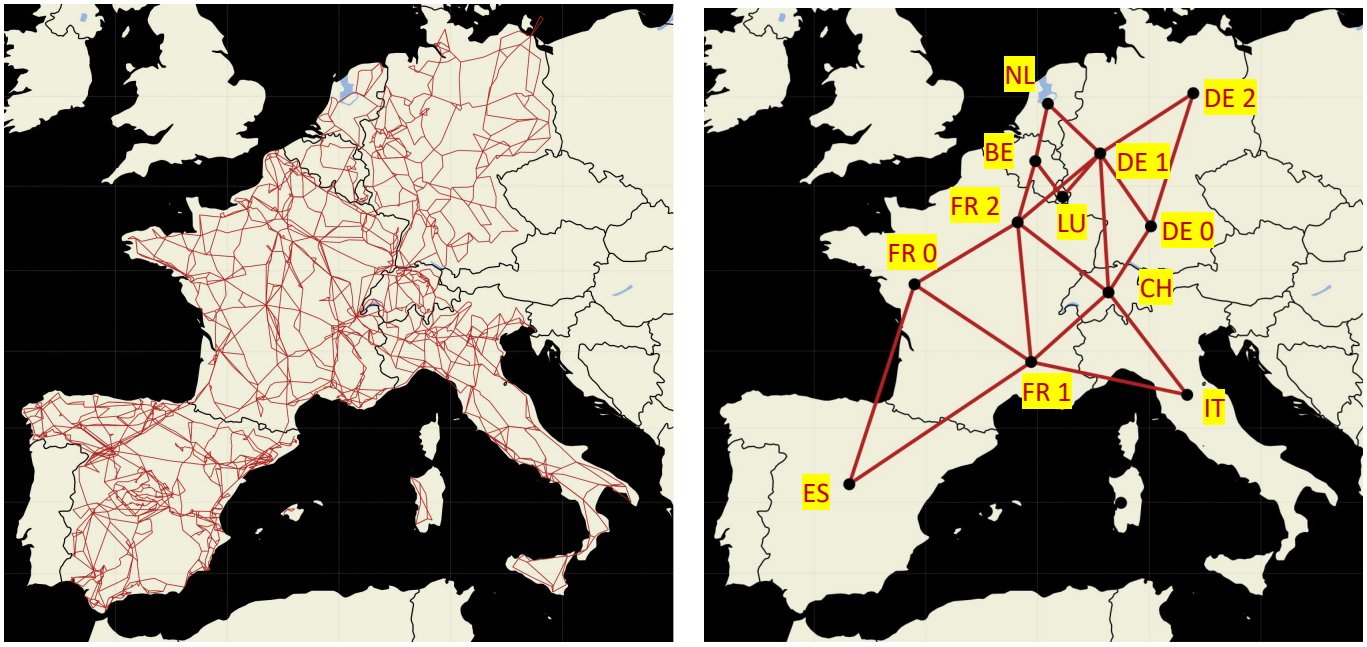

(a) Full power network for the set of European countries selected.

(b) Equivalent power system after applying clustering to calculate an equivalent reduced number of buses and transmission lines.

Figure 5: Power system considered for the case study.

For the set of countries considered in the case study, the full power system consists of 2069 buses distributed among countries, and 3154 HVAC transmission lines connecting them. The full power system is illustrated in Figure (5a). For long-term generation expansion planning at this scale, it is not practical to consider every bus in the system. It is very common for studies in the literature to aggregate the generation buses based on administrative boundaries such as country borders to significantly reduce the size of the network considered (Rodriguez et al., 2014; Gils et al., 2017; Victoria et al., 2020; Pavičević et al., 2020). PyPSA-Eur itself consists of a power system optimization-based planning model that uses a number of clustering techniques to significantly reduce the size of the network. Moreover, as previously noted, unlike most planning models in the literature, the scope of our model is different since it considers explicit integer formulation for the investment decisions and the integration of the unit

commitment problem within the optimization framework, as well as, the modeling of the uncertainties of the load and IRES-CF. We, thus, similarly implement the clustering method proposed in (Hörsch and Brown, 2017) to reduce the network size to a computationally manageable -yet representative- equivalent system. The equivalent power system shown in Figure (5b) consists of 12 buses distributed along the 8 selected countries and 20 equivalent 380kV transmission lines connecting them. The clustering method used groups close-by buses together, so that, multiple buses representing neighboring cities are merged into one bus. Buses from different synchronous zones are not merged together to maintain the realistic representation of transmission corridors between separate synchronous zones.

Table (7) summarizes the transmission lines technical characteristics for the equivalent power system shown in Figure (5b). Each line is indicated based on the nodes it connects and characterized by the inductance, the number of parallel circuits installed and the total power carrying capacity it can transmit between the two nodes. The number of generation units existing at the beginning of the planning horizon at each node is given in Table (8a). These numbers of units are calculated based on the data for the total existing capacity at each node, obtained from the PPM database, divided by the maximum generation capacity per unit considered in this paper, shown in Table (2).

Here, we also consider a number of representative days to characterize the future planning year. In particular, we consider 4 uncertain days to represent a range of time series for wind and solar capacity factors and for the power demand. Figure (6) illustrates an example for one selected day for the capacity factor of wind (Figure (6a)) and solar (Figure (6b)) at each bus. It can be seen that, even for one selected day, a wide range of wind and solar profiles are covered for consideration in the planning process. Moreover, since the MS-AARC model proposed considers the uncertainty in wind and solar availability, Figure (7) illustrates an example of one wind and one solar profiles and the uncertainty range considered for each. Notice that the robust MS-AARC model provides a solution that is feasible for all the uncertainty realizations

Table 7: Transmission lines characteristics

From i	To j	Total transmission capacity [MW] $\bar{f}_{ij}$	Reactance [Ohm] $\mathcal{X}_{ij}$	Number of parallel circuits
BE	FR2	11,327	63.07	7
BE	LU	1,138	44.13	1
CH	NL	6,792	56.09	4
CH	DE0	16,981	80.86	10
CH	DE1	3,396	140.44	2
CH	FR1	10,207	111.25	6
CH	FR2	3,380	117.89	2
CH	IT	8,500	139.46	5
DE0	DE1	34,541	87.76	20
DE0	DE1	11,887	135.58	7
DE1	DE2	14,723	105.07	9
DE1	FR2	9,629	106.01	6
DE1	LU	3,984	56.27	2
DE1	NL	6,792	68.63	4
ES	FR0	2,836	232.49	2
ES	FR1	1,698	246.82	1
FR0	FR1	13,044	149.44	8
FR0	FR2	23,802	123.25	14
FR1	FR2	22,085	147.34	13
FR1	IT	5,663	175.12	3

of wind and solar capacity factor in the uncertainty range, i.e., for all the possible combination of points within the shaded areas. This, indeed, accounts for a significant number of wind and solar capacity factors, as well as, load profiles in the model.

6.2. Results and analysis: multi-regional generation expansion planning with operational uncertainty

The proposed MS-AARC model is used to solve the case study based on the European system described in the previous section. The case study is solved for a number of scenarios covering different targets for renewable penetration levels in the system expansion: (i) IRES = 25%; (ii) IRES = 50% and (iii) IRES = 75%. For each renewable penetration level, three levels of uncertainty ranges in the hourly renewable capacity factor and power demand at each node are considered, these uncertainty ranges, de-

Table 8: Number of generation units/generation capacity existing at each node (number of unites calculated as the total existing capacity divided by the maximum generation capacity per unit considered in Table (2))

(a) Number of generation units

Technology	[BE]	[CH]	[DE0]	[DE1]	[DE2]	[ES]	[FR0]	[FR1]	[FR2]	[IT]	[LU]	[NL]
Nuclear	5	3	4	6	2	6	13	10	23	1	0	1
Coal	2	4	3	18	6	6	2	1	2	9	0	6
CCGT	7	11	7	22	6	45	1	4	7	64	1	25
On-Shore Wind	9	1	42	63	81	100	19	11	13	36	1	15
Solar-PV	18	7	66	72	82	27	13	10	10	103	1	12

(b) Total installed capacity [in GW]

Technology	[BE]	[CH]	[DE0]	[DE1]	[DE2]	[ES]	[FR0]	[FR1]	[FR2]	[IT]	[LU]	[NL]
Nuclear	7.00	4.20	5.60	8.40	2.80	8.40	18.20	14.00	32.20	1.40	0.00	1.40
Coal	2.20	4.40	3.30	19.80	6.60	6.60	2.20	1.10	2.20	9.90	0.00	6.60
CCGT	3.85	6.05	3.85	12.10	3.30	24.75	0.55	2.20	3.85	35.20	0.55	13.75
On-Shore Wind	2.16	0.24	10.08	15.12	19.44	24.00	4.56	2.64	3.12	8.64	0.24	3.60
Solar-PV	3.24	1.26	11.88	12.96	14.76	4.86	2.34	1.80	1.80	18.54	0.18	2.16

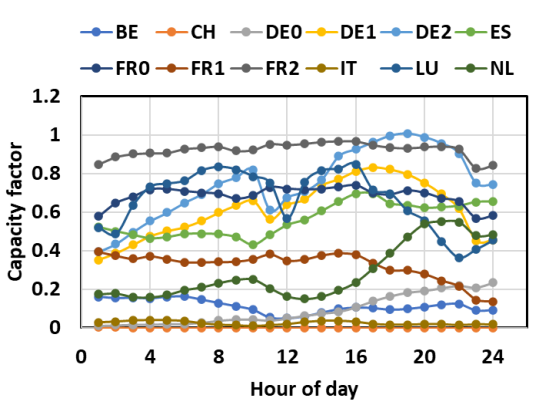

(a) On-shore Wind

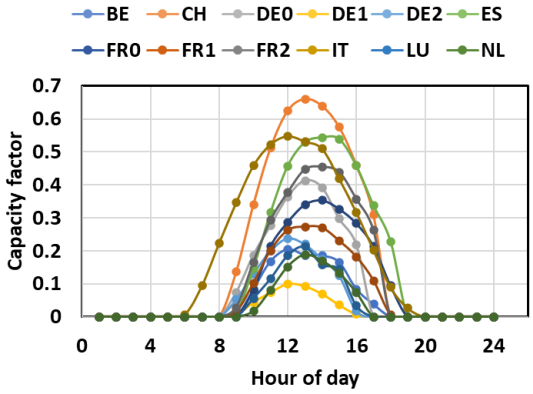

(b) PV-Solar

Figure 6: Example of one representative day (24 hours) of the capacity factor of wind and solar energy at each generation bus.

noted as UR, are calculated as percentage variations around the hourly nominal values. The uncertainty ranges considered are: (i) no uncertainty (UR= ± 0);(ii) 20% range of uncertainty around the nominal value (UR= $\pm 10\%$) and (iii) 50% range of uncertainty

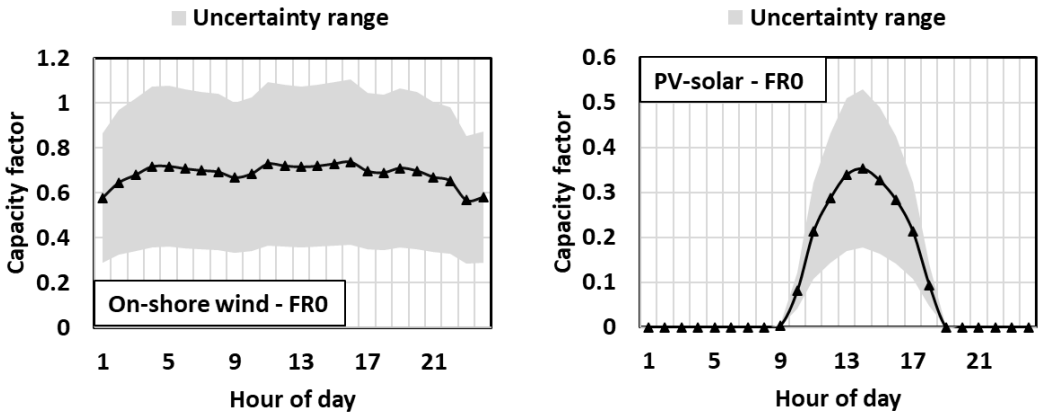

(a) On-shore Wind

(b) PV-Solar

Figure 7: Example of the uncertainty range considered for the capacity factors of renewable resources at bus FR0. Notice that the robust MS-AARC model gives a solution that is feasible for every possible combination of all the points of the shaded areas.

around the nominal value (UR= $\pm 25\%$).

6.2.1. Investment capacities and generation mix

Figure (8) shows the breakdown of the the generation capacities existing in the power system before any expansion. The total installed capacity is around 448GW distributed roughly equally among Nuclear (23.12%), CCGT (24.55%) and Wind (20.94%) capacities, and to a lesser extent Coal (14.48%) and Solar (16.91%) capacities. As can be seen in the figure, nuclear capacity is primarily concentrated in the nodes in France, while wind and solar capacities are primarily concentrated in the European south at Italy and Spain, and the northwestern nodes in Germany.

Figure (9) shows the breakdown of generation investment as per the solution of the MS-AARC model, for the different scenarios of IRES penetration level (moving vertically along the graphs) and the different scenarios of uncertainty ranges (moving horizontally along the graphs). First, in terms of the total capacity installed, notice the significant increase in capacity compared to the initial system before expansion. For the lowest IRES penetration scenario, the capacity installed almost doubles from 448.12 GW in the initial system to around 1082.78GW for the expansion plan obtained

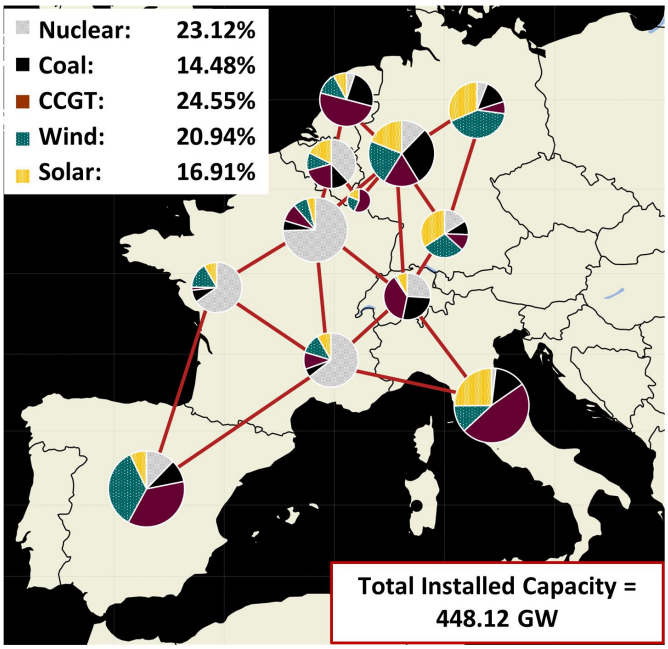

Figure 8: Breakdown of generation capacity per technology and their distribution in the power system before expansion.

at IRES = 25% and no consideration of uncertainty (Figure (9a)). This is, on one hand, due to the assumed increase in the system load, as discussed in the previous section, and, on the other hand, due to the requirement to satisfy a percentage of the load using renewable technologies, which generally have a lower output per MW installed.

As seen in Figure (9), the investment capacities increase when the uncertainty in IRES-CF and system load are considered. For example, for the case of 25% IRES penetration, there is an increase of 112GW and 341.2GW for the solutions considering an uncertainty range of ±10% (Figure (9b)) and ±25% (Figure (9c)), respectively, compared to when no uncertainty is considered. A similar increase can be observed for the other scenarios of IRES penetration, notably 50% and 75% IRES levels, when the uncertainty ranges are increased. These differences in the total capacity installed can be observed on Figures (9d) to (9f) for IRES = 50% and Figures (9g) to (9i) for IRES = 75%.

The total capacity increase for the uncertain scenarios is expected since the renew-

able capacity installed should be robust to the realization of lower capacity factors. Moreover, the whole system is dimensioned adequately, with enough fast ramping generation units online, capable of handling the ramping uncertainties.

In addition to the total installed capacity, the generation mix resulting for each scenario clearly reflects the respective policy choice. More wind and solar capacities are installed when considering uncertainty in the system operation. As an example for the scenario of 50% IRES penetration, the share of wind capacity in the system increases from 58.87% if no uncertainty is considered ((Figure (9d))) to 62.97% and 67.62% for the UR of ±10% (Figure (9e)) and ±25% (Figure (9f)), respectively. Notice that this increase also coincides with the overall increase in the total capacity of the system. Fossil technologies, on the other hand, maintain a relatively constant share across the different uncertain scenarios, and provide a counterbalance to the operational uncertainty of the system because of their dispatchable nature.

Finally, notice that the total installed capacity in the system increases significantly as the IRES penetration level increases (i.e. moving vertically in Figure (9). For example, for the case of UR: ±25% (Figures (9c), (9f), (9i)), the total capacity slightly increases from 1424.2GW to 1440.2GW for 25% to 50% IRES, while it significantly increases to around 3186.96GW for the scenario enforcing 75% IRES penetration. This significant increase highlights the non-linear nature of capacity investment required to increase the renewable levels in the system. Indeed, in all scenarios optimized, the results indicate that increasing the IRES penetration to 75% more than doubles the capacity required compared to a system with 50% renewable penetration. In addition, the generation mix heavily shifts towards renewable and is significantly reduced for the fossil and nuclear technologies. Notice in Figure (9) how the combined effect of considering uncertainty and a high penetration of IRES (moving to the right and down) shifts the mix heavily towards wind and solar power, and to a lesser extent nuclear, at the expense of the fossil technologies.

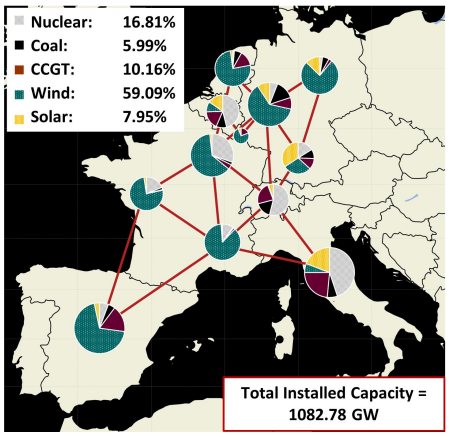

(a) IRES = 25%, UR: ± 0%

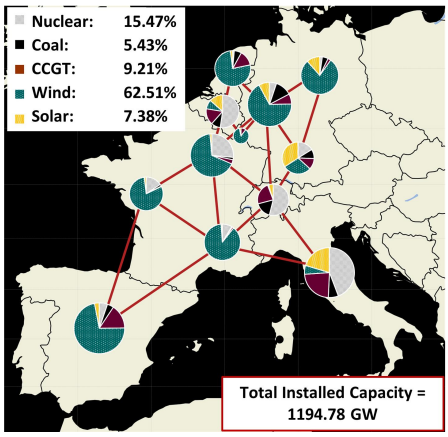

(b) IRES = 25%, UR: ± 10%

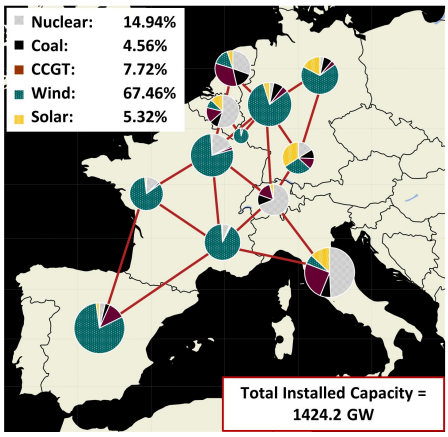

(c) IRES = 25%, UR: ± 25%

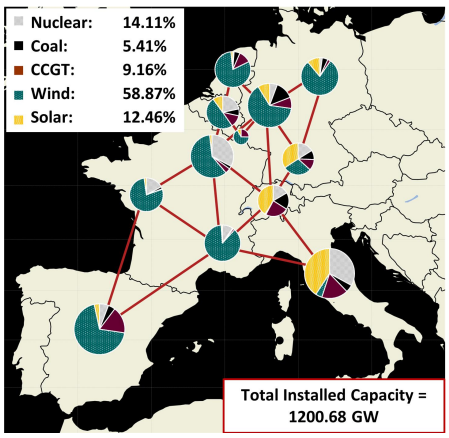

(d) IRES = 50%, UR: ± 0%

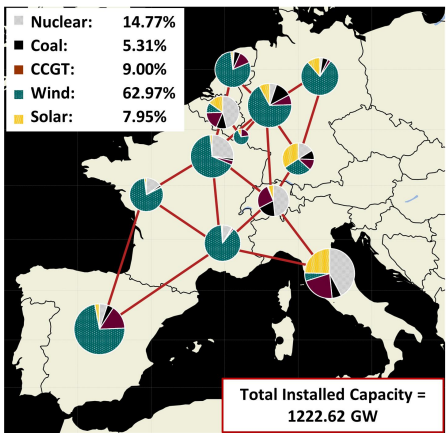

(e) IRES = 50%, UR: ± 10%

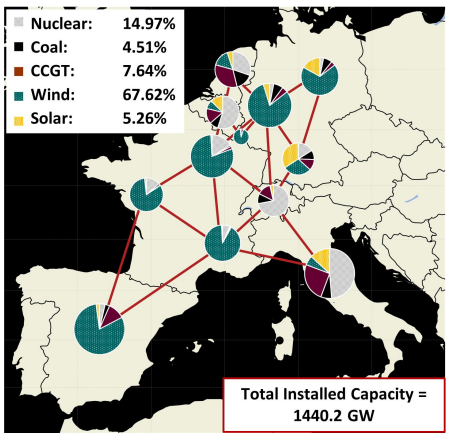

(f) IRES = 50%, UR: ± 25%

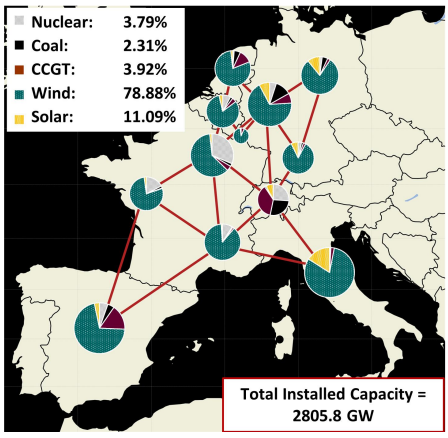

(g) IRES = 75%, UR: ± 0%

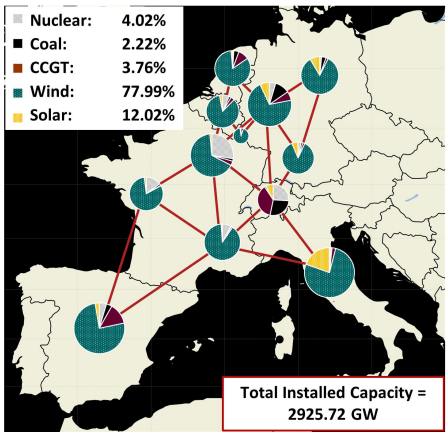

(h) IRES = 75%, UR: ± 10%

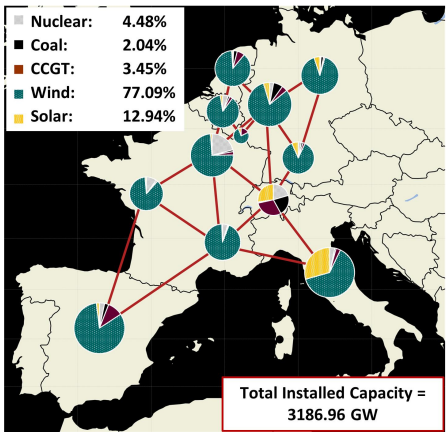

(i) IRES = 75%, UR: ± 25%

Figure 9: Breakdown of generation capacity per technology and their distribution in the power system for different expansion scenarios.

6.2.2. Investment costs

The results for the investment costs reflects similar trends previously observed for the investment capacities. Figure (10) illustrates the results for the total investment costs (in Billion Euros) for all IRES and UR scenarios considered, as well as, a breakdown for the IRES share of investment costs and percentages across scenarios.

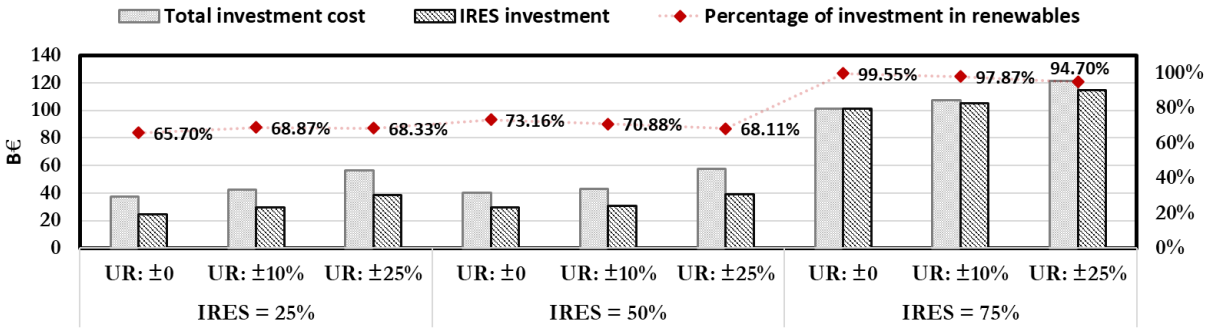

Figure 10: Results for the total investment costs (in Billion Euros) for all IRES and UR scenarios considered + IRES share of investment costs and percentages across scenarios.

As expected, considering uncertainty leads to an increase in the total investment costs in the system. This is primarily due to the increase in the renewable capacity installed, as seen in the previous section. The total investment cost for the case of 25% IRES increase from 34.43B€to 42.72 B€and 56.47B€, for the cases of UR: ±0%, UR: ±10% and UR: ±25%, respectively. This represents an increase of 5.28B€and 19.04B€compared to the base-case scenario with no uncertainty. Similar increases are observed for the different uncertain scenarios of the 50% IRES and 75% IRES cases.

Notice how the significant increase in capacities installed for the 75% IRES scenario observed in the previous section is reflected in the investment costs seen in Figure (10). Compared to the average investment costs of around 45B€and 47B€for the 25% IRES and 50% IRES cases, respectively, the 75% IRES case results in an average investment cost of 110B€across UR scenarios; more than double of that of the other penetration levels.

Renewable sources represent a significant percentage of the investment costs for all scenarios considered as can be seen in the scatter plot in Figure (10). For the 25%

and 50% IRES cases, the percentage of IRES investments reaches levels of 68.87% and 73.16% of the total new investments, respectively. The percentage of renewable investments in the 75% IRES case represents almost the entirety of the new total investments, going up to 99.55%, as can be seen in the figure.

Notice the slight decrease in the respective percentage of IRES investments as the UR increases for the 50% and 75% IRES cases. The percentage of IRES investments decrease from 73.16% for UR: ±0% to 68.11% for UR: ±10% for the 50% IRES case. Similarly, the percentage of IRES investments decrease from 99.55% for UR: ±0% to 94.70% for UR: ±10% for the 75% IRES case. This can be explained by observing that, as the uncertainty in the system increases, more dispatchable units are required in the system to ensure its operational flexibility against the ramping uncertainty. In our results, this is reflected in more nuclear units installed across these uncertain scenarios. While these results may depend on the characteristics assumed for the generation units (for example the ramping rates and minimum up and down times, etc.), the overall observation for the need of more conventional units to hedge against the operational uncertainty should remain valid.

6.2.3. IRES shedding

Figure (11) summarizes the IRES shedding amount assuming the system is operated under the worst-case hourly capacity factor realization as given by the MS-AARC model. Notice that, as previously explained, the worst-case uncertainty realization cannot be readily estimated to be the lowest capacity factor for the renewable energy at every hour. Instead, this has been shown to be driven by less obvious interactions of ramping uncertainties that are explicitly considered within the proposed MS-AARC framework. The multistage nature of the model ensures that time-coupling uncertainty, between each time step and the next, is properly accounted for.

The results show how the percentage of IRES shedding in the system increases as the IRES level in the system increases. For example, for the case without considering any uncertainty, IRES shedding reaches levels of 8.16%, 11.53% and 19.54% for the

25%, 50% and 75% IRES scenarios, respectively. Notice, however, how these shedding values *decrease* as the model is solved considering uncertainties. As seen in Figure (11), for the 25% IRES scenario, the shedding percentage decrease from 8.16% to 5.69% and down to 3.02% for the UR: ±0%, UR: ±10% and UR: ±25%, respectively. Similar trends are observed for the other IRES penetration levels as can be seen in the figure.

First, recall that the total renewable capacity in the system is higher for the results considering higher uncertainty levels. Moreover, the generation mix in the respective cases is optimized by the MS-AARC model to handle the uncertainty, for example, by adding more conventional units that can provide base load or ramp quickly. The lower IRES shedding is, thus, a result of an overall higher investment in the system capacity and the generation mix to properly account for the uncertainties.

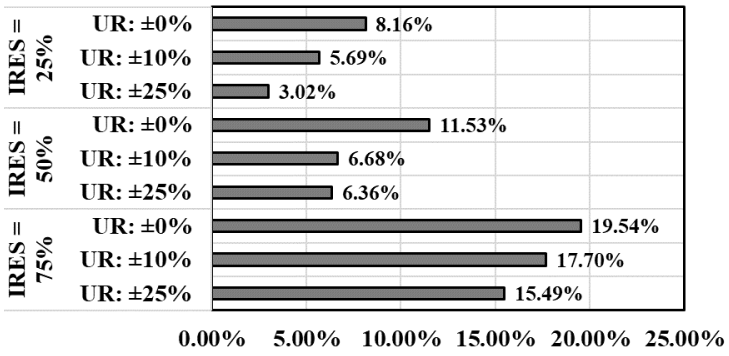

Figure 11: Total IRES shedding in the power system for each scenario considered.

While the IRES shedding is not explicitly optimized in the model (it could be easily incorporated as an objective in the optimization), these results can help the policymaker evaluate the possible benefit of the different investment schemes and generation mixes obtained from the MS-AARC in accounting for different levels of system uncertainties.

6.2.4. Transmission lines utilization and congestion.

Power flow in the transmission lines connecting the different buses has an important effect on the generation capacities installed at each bus. Indeed, if lines are not ade-

quately dimensioned, the congestion in those lines may lead to sub-optimal generation investments at nodes on both ends of the connection. While transmission expansion planning is beyond the scope of this paper, it can be easily incorporated in the MS-AARC optimization model proposed. However, here we show the model capability in providing insights into identifying congested lines and their impact on generation expansion planning.

Hourly power flows in each transmission line are obtained from the MS-AARC model solution. These results are studied to identify lines that are loaded at, or close to, their maximum carrying capacities. Lines that are consistently operated at their maximum carrying capacities can be regarded, with high confidence, as congested lines that can be a subject of transmission expansion consideration.

Figure (12) illustrate an example of selected transmission lines that are consistently operating near to or at their maximum capacities for the 50% IRES penetration scenario. The illustration is for the power flow during the day with the highest average IRES capacity factor. Each graph, also, groups the results obtained for the solution under different uncertainty level. As seen in the figure, the selected lines: 2, 7 and 16, are operating at their maximum capacities for more than 18 to 23 hours of the daily operations. There is a significant probability that those lines, and similarly performing ones, represent a bottle neck for power transmission that can reduce the overall system costs if adequately treated. Such an investigation can be a relevant extension for the results shown here.

7. Conclusions

The proper treatment of uncertainties in planning future electric power systems is critical for policymakers and practitioners. Generation expansion planning models with a high share of intermittent renewable energy penetration must be able to account for both short-term inter-temporal variability and uncertainty in renewable production and load levels. To address this issue, this paper proposes a novel multistage robust optimization model for the integrated generation expansion planning and unit-commitment

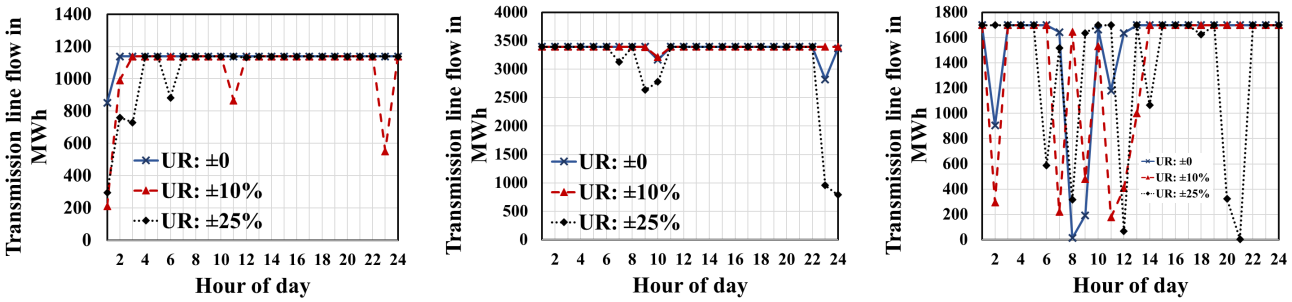

(a) Line 2: BE to LU

(b) Line 7: CH to FR2

(c) Line 16: ES to FR1

Figure 12: Example of power flow level in selected transmission lines (most congested) for the 50% IRES penetration scenario and considering different uncertainty levels.

(IGEP-UC) problem. Different from two-stage robust or stochastic models, multistage robust optimization allows the sequential representation of uncertainty realizations as they are revealed over time. It also considers the non-anticipativity of future uncertainty realizations at the time of decision-making, which is the case in practical real-world applications. Moreover, the IGEP-UC problem formulated is multi-period, i.e. spanning several years, and mutli-regional, i.e. considering different investment locations and the transmission network connecting them. The integrated unit-commitment problem means that the short-term characteristics of the system, such as the start-up and shut-down of units and the their ramping capacities, is explicitly considered in the planning model. We develop a tractable form of the multistage robust model and propose a solution method relying on the reduction of the information basis of the decision rules that map the uncertainty realizations to the changes in recourse variables.

We, first, validate the performance of the proposed solution method on a reduced-size case study, and show that the model is computationally tractable and that significant gains in computational times can be achieved by the proposed information basis reduction, while maintaining the quality of the solution. In particular, we show that the results of the results obtained by the proposed reduction approach are within 1% at most compared to the results obtained from the non-reduced problem. Thereof ensuring that the results remain optimal within a very low tolerance, with significant

gains in computational time.

Moreover, a comprehensive analysis on a case-study based on the European power system spanning 8 European countries is presented. The results obtained show the model capability in providing useful insights to the investment decisions, in terms of generation mix, renewable shedding, power flow in the transmission lines, among others. Moreover, we show the importance of considering the short-term uncertainties of the system load and renewable production in a multistage setting, and how those uncertainties re-define the worst-case operational requirements in such a way that would not be captured within non-causal planning models.

It should be noted that a number of important assumptions have been made in this work. Most notably, the use of a limited number of representative days to account for net-load variations, the use of the integer clustering method for handling identical generation units and the assumption of linear relationships in the model formulation. To best of our capabilities, all our assumptions are made based on validated methods in the literature that have investigated their effectiveness and validated their relevance for solving power system planning problems. However, it should be highlighted that, while these assumptions are made with the aim of ensuring a high quality tractable solution to the large-scale planning problem under uncertainty, a more in-depth analysis is required to identify their limitations towards real application. This will be considered in future improvements of this work.

Moreover, future extensions of this work may consider the treatment of long-term uncertainties in system planning, such as fuel prices or investment costs or policy incentive schemes. Another relevant extension is the consideration of finer temporal resolution for the net-load variation as, in our work, only hourly resolution have been considered. Sub-hourly resolution might be relevant particularly since the availability of renewable energy sources might vary significantly in shorter periods of time. Finally, since our focus in this work is the generation expansion problem, decisions for transmission grid expansion may, also, be integrated to the uncertain planning problem in future extensions.

Acknowledgment

The authors would like to thank Dr. Elizaveta Kuznetsova for her feedback and support in the early stages of the work. This work was partially supported by the Future Resilient Systems project at the Singapore-ETH Center (SEC), which is funded by the National Research Foundation of Singapore (NRF), Prime Minister's Office, Singapore, under its Campus for Research Excellence and Technological Enterprise (CREATE) program. The project is administered by the National University of Singapore (NUS) under grants WBS R-266-000-089-592 and R-266-000-070-281.

References

Sérgio Pereira, Paula Ferreira, and A Ismael F Vaz. Generation expansion planning with high share of renewables of variable output. *Applied energy*, 190:1275–1288, 2017.

Athanasios S Dagoumas and Nikolaos E Koltsaklis. Review of models for integrating renewable energy in the generation expansion planning. *Applied Energy*, 242:1573–1587, 2019.

MI Alizadeh, M Parsa Moghaddam, N Amjady, P Siano, and MK Sheikh-El-Eslami. Flexibility in future power systems with high renewable penetration: A review. *Renewable and Sustainable Energy Reviews*, 57:1186–1193, 2016.

Jia Li, Feng Liu, Zuyi Li, Chengcheng Shao, and Xinyuan Liu. Grid-side flexibility of power systems in integrating large-scale renewable generations: A critical review on concepts, formulations and solution approaches. *Renewable and Sustainable Energy Reviews*, 93: 272–284, 2018a.

Paul Neetzow. The effects of power system flexibility on the efficient transition to renewable generation. *Applied Energy*, 283:116278, 2021.

Philipp Andreas Gunkel, Claire Bergaentzlé, Ida Græsted Jensen, and Fabian Scheller. From passive to active: Flexibility from electric vehicles in the context of transmission system development. *Applied Energy*, 277:115526, 2020.

Bryan Palmintier and Mort Webster. Impact of unit commitment constraints on generation expansion planning with renewables. In *2011 IEEE power and energy society general meeting*, pages 1–7. IEEE, 2011.

Nikolaos E Koltsaklis and Michael C Georgiadis. A multi-period, multi-regional generation expansion planning model incorporating unit commitment constraints. *Applied energy*, 158:310–331, 2015.

Islam F Abdin and Enrico Zio. An integrated framework for operational flexibility assessment in multi-period power system planning with renewable energy production. *Applied Energy*, 222:898–914, 2018.

Xuan Zhang and Antonio J Conejo. Robust transmission expansion planning representing long-and short-term uncertainty. *IEEE Transactions on Power Systems*, 33(2):1329–1338, 2017.

NREL National Renewable Energy Laboratory U.S. and United States. Department of Energy. Office of Scientific and Technical Information. *ERCOT Event on February 26, 2008: Lessons Learned*. United States. Department of Energy, 2008. URL `https://books.google.fr/books?id=_6ctuwEACAAJ`.

Richard G Smead. Ercot—the eyes of texas (and the world) are upon you: What can be done to avoid a february 2021 repeat. *Climate and Energy*, 37(10):14–18, 2021.

Nikolaos E Koltsaklis and Konstantinos Nazos. A stochastic milp energy planning model incorporating power market dynamics. *Applied Energy*, 205:1364–1383, 2017.

Heejung Park and Ross Baldick. Stochastic generation capacity expansion planning reducing greenhouse gas emissions. *IEEE Transactions on Power Systems*, 30(2):1026–1034, 2015.

Hao Quan, Dipti Srinivasan, Ashwin M Khambadkone, and Abbas Khosravi. A computational framework for uncertainty integration in stochastic unit commitment with intermittent renewable energy sources. *Applied energy*, 152:71–82, 2015.

Jiadong Wang, Jianhui Wang, Cong Liu, and Juan P Ruiz. Stochastic unit commitment with sub-hourly dispatch constraints. *Applied energy*, 105:418–422, 2013.

Jiaying Shi and Shmuel S Oren. Stochastic unit commitment with topology control recourse for power systems with large-scale renewable integration. *IEEE Transactions on Power Systems*, 33(3):3315–3324, 2018.

Cong Chen, Hongbin Sun, Xinwei Shen, Ye Guo, Qinglai Guo, and Tian Xia. Two-stage robust planning-operation co-optimization of energy hub considering precise energy storage economic model. *Applied energy*, 252:113372, 2019.

Aakil M Caunhye and Michel-Alexandre Cardin. Towards more resilient integrated power grid capacity expansion: A robust optimization approach with operational flexibility. *Energy Economics*, 72:20–34, 2018.

Stefano Moret, Frédéric Babonneau, Michel Bierlaire, and François Maréchal. Overcapacity in european power systems: Analysis and robust optimization approach. *Applied Energy*, 259:113970, 2020.

Esnil Guevara, Fréderic Babonneau, Tito Homem-de Mello, and Stefano Moret. A machine learning and distributionally robust optimization framework for strategic energy planning under uncertainty. *Applied Energy*, 271:115005, 2020.

Bo Zhou, Xiaomeng Ai, Jiakun Fang, Wei Yao, Wenping Zuo, Zhe Chen, and Jinyu Wen. Data-adaptive robust unit commitment in the hybrid ac/dc power system. *Applied Energy*, 254:113784, 2019.

Hongxing Ye and Zuyi Li. Robust security-constrained unit commitment and dispatch with recourse cost requirement. *IEEE Transactions on Power Systems*, 31(5):3527–3536, 2016.

Dimitris Bertsimas, Eugene Litvinov, Xu Andy Sun, Jinye Zhao, and Tongxin Zheng. Adaptive robust optimization for the security constrained unit commitment problem. *IEEE Transactions on Power Systems*, 28(1):52–63, 2013.

Álvaro Lorca, X Andy Sun, Eugene Litvinov, and Tongxin Zheng. Multistage adaptive robust optimization for the unit commitment problem. *Operations Research*, 64(1):32–51, 2016.

Alvaro Lorca and Xu Andy Sun. Multistage robust unit commitment with dynamic uncertainty sets and energy storage. *IEEE Transactions on Power Systems*, 32(3):1678–1688, 2017.

Jinye Zhao, Tongxin Zheng, and Eugene Litvinov. A unified framework for defining and measuring flexibility in power system. *IEEE Transactions on Power Systems*, 31(1):339–347, 2015.

Jinye Zhao, Tongxin Zheng, and Eugene Litvinov. Variable resource dispatch through do-not-exceed limit. *IEEE Transactions on Power Systems*, 30(2):820–828, 2014.

Jia Li, Zuyi Li, Feng Liu, Hongxing Ye, Xuemin Zhang, Shengwei Mei, and Naichao Chang. Robust coordinated transmission and generation expansion planning considering ramping requirements and construction periods. *IEEE Transactions on Power Systems*, 33(1):268–280, 2018b.

Felipe Verastegui, Alvaro Lorca, Daniel E Olivares, Matias Negrete-Pincetic, and Pedro Gazmuri. An adaptive robust optimization model for power systems planning with operational uncertainty. *IEEE Transactions on Power Systems*, 2019.

Alexandre Velloso, David Pozo, and Alexandre Street. Distributionally robust transmission expansion planning: a multi-scale uncertainty approach. *IEEE Transactions on Power Systems*, 35(5):3353–3365, 2020.

Shahab Dehghan, Nima Amjady, and Antonio J Conejo. A multistage robust transmission expansion planning model based on mixed binary linear decision rules—part i. *IEEE Transactions on Power Systems*, 33(5):5341–5350, 2018.

Yixian Liu, Ramteen Sioshansi, and Antonio J Conejo. Multistage stochastic investment planning with multiscale representation of uncertainties and decisions. *IEEE Transactions on Power Systems*, 33(1):781–791, 2018.

Alexander Shapiro and Arkadi Nemirovski. On complexity of stochastic programming problems. In *Continuous optimization*, pages 111–146. Springer, 2005.

Aharon Ben-Tal, Alexander Goryashko, Elana Guslitzer, and Arkadi Nemirovski. Adjustable robust solutions of uncertain linear programs. *Mathematical Programming*, 99(2):351–376, 2004.

Bryan S Palmintier and Mort D Webster. Heterogeneous unit clustering for efficient operational flexibility modeling. *IEEE Transactions on Power Systems*, 29(3):1089–1098, 2014.

Daniel Kuhn, Wolfram Wiesemann, and Angelos Georghiou. Primal and dual linear decision rules in stochastic and robust optimization. *Mathematical Programming*, 130(1):177–209, 2011.

RTE-France. Available at:. http://clients.rte-france.com, 2017. (Accessed on 20-10-2018).

Karl E Taylor, Ronald J Stouffer, and Gerald A Meehl. An overview of cmip5 and the experiment design. *Bulletin of the American Meteorological Society*, 93(4):485–498, 2012.

Kris Poncelet, Hanspeter Höschle, Erik Delarue, Ana Virag, and William D'haeseleer. Selecting representative days for capturing the implications of integrating intermittent renewables in generation expansion planning problems. *IEEE Transactions on Power Systems*, 32(3): 1936–1948, 2017.

IEA/NEA. Projected costs of generating electricity 2015 edition. *OECD*, 2015.

William E Hart, Carl Laird, Jean-Paul Watson, and David L Woodruff. *Pyomo–optimization modeling in python*, volume 67. Springer Science & Business Media, 2012.

Jonas Hörsch, Fabian Hofmann, David Schlachtberger, and Tom Brown. Pypsa-eur: An open optimisation model of the european transmission system. *Energy Strategy Reviews*, 22:207–215, 2018.

ENTSO-E. European network of transmission system operators for electricity. ten-yead network development plan (tyndp) 2018. 2018.

OPSD. Load in hourly resolution, 2019. https://open-power-system-data.org/, 2019. (Accessed on 20-11-2020).

Fabian Hofmann and Jonas Hörsch. FRESNA/powerplantmatching: powerplantmatching v.0.4.1, August 2019. URL `https://doi.org/10.5281/zenodo.3358985`.

Hans Hersbach, Bill Bell, Paul Berrisford, Shoji Hirahara, András Horányi, Joaquín Muñoz-Sabater, Julien Nicolas, Carole Peubey, Raluca Radu, Dinand Schepers, et al. The era5 global reanalysis. *Quarterly Journal of the Royal Meteorological Society*, 146(730):1999–2049, 2020.

Martha Maria Frysztacki, Jonas Hörsch, Veit Hagenmeyer, and Tom Brown. The strong effect of network resolution on electricity system models with high shares of wind and solar. *Applied Energy*, 291:116726, 2021.

Rolando A Rodriguez, Sarah Becker, Gorm B Andresen, Dominik Heide, and Martin Greiner. Transmission needs across a fully renewable european power system. *Renewable Energy*, 63:467–476, 2014.

Hans Christian Gils, Yvonne Scholz, Thomas Pregger, Diego Luca de Tena, and Dominik Heide. Integrated modelling of variable renewable energy-based power supply in europe. *Energy*, 123:173–188, 2017.

Marta Victoria, Kun Zhu, Tom Brown, Gorm B Andresen, and Martin Greiner. Early decarbonisation of the european energy system pays off. *Nature communications*, 11(1):1–9, 2020.

Matija Pavičević, Andrea Mangipinto, Wouter Nijs, Francesco Lombardi, Konstantinos Kavvadias, Juan Pablo Jiménez Navarro, Emanuela Colombo, and Sylvain Quoilin. The potential of sector coupling in future european energy systems: Soft linking between the dispa-set and jrc-eu-times models. *Applied Energy*, 267:115100, 2020.

Jonas Hörsch and Tom Brown. The role of spatial scale in joint optimisations of generation and transmission for european highly renewable scenarios. In *2017 14th international conference on the European Energy Market (EEM)*, pages 1–7. IEEE, 2017.

Appendix A. IGEP-UC deterministic model formulation

Objective function

$$\min_{\boldsymbol{\Omega},\boldsymbol{\Theta}} \sum_{y\in Y}\sum_{i\in I}(1+DF)^{-y}\cdot\Bigg[\sum_{g\in G^{(new)}} Inv\_C_g\cdot\bar{P}_g\cdot q_{ig}^{y} \tag{A.1a}$$

$$+\sum_{g\in G} C_g^{OM}\cdot\bar{P}_g\cdot\sum_{l=1}^{y} q_{ig}^{l} \tag{A.1b}$$

$$+\sum_{s\in S}\sum_{t\in T}\sum_{g\in G^{(th)}}\Big(St\_C_g\cdot z_{ig}^{yst}\Big) \tag{A.1c}$$

$$+\sum_{s\in S}\sum_{t\in T}\Big[\sum_{g\in G}\Big(Marg\_C_g^{y}\cdot p_{ig}^{yst}\Big)+Lns\_C\cdot lns_i^{yst}\Big]\Bigg] \tag{A.1d}$$

where $\boldsymbol{\Omega}=\{\boldsymbol{q},\ \boldsymbol{x},\ \boldsymbol{u},\ \boldsymbol{z},\ \boldsymbol{v}\}$ is the set of the investment and commitment decision variables and $\boldsymbol{\Theta}=\{\boldsymbol{p},\ \boldsymbol{lns},\ \boldsymbol{f},\ \boldsymbol{\theta}\}$ is the set of generation and network power dispatch variables, respectively.

IGEP-UC model constraints

The minimization of the objective is subject to long-term investment constraints, and short-term hourly unit commitment and dispatch constraints as follows:

investment and commitment constraints

$$x_{ig}^{y}\le\sum_{l=1}^{y} q_{ig}^{l},\quad \forall i\in I, g\in G^{(new)}, y\in Y \tag{A.2a}$$

$$\sum_{i\in I^c}\sum_{g\in G^{(new)}} Inv\_C_g\cdot\bar{P}_g\cdot q_{ig}^{y}\le Inv\_Max^{y},\quad \forall y\in Y \tag{A.2b}$$

$$\sum_{i\in I^c}\sum_{g\in G^{(th)}}\Big(\bar{P}_g\cdot x_{ig}^{y}\Big)\ge\Big(1+r^{(min)}\Big)\cdot L^{Max},\quad \forall y\in Y \tag{A.2c}$$

$$u_{ig}^{yst}\le x_{ig}^{y},\quad \forall i\in I, g\in G^{(th)}, y\in Y, s\in S, t\in T \tag{A.2d}$$

$$u_{ig}^{yst}-u_{ig}^{yst-1}=z_{ig}^{yst}-v_{ig}^{yst},\quad \forall i\in I, g\in G^{(th)}, y\in Y, s\in S, t\in T\setminus\{1\} \tag{A.2e}$$

$$u_{ig}^{yst}\ge\sum_{\tau\ge t-UM_g}^{t} z_{ig}^{ys\tau},\quad \forall i\in I, g\in G^{(th)}, y\in Y, s\in S, t\in T\setminus\{1,...,UM_g\} \tag{A.2f}$$

$$x_{ig}^{y}-u_{ig}^{yst}\ge\sum_{\tau\ge t-DM_g}^{t} v_{ig}^{ys\tau}, \forall i\in I, g\in G^{(th)}, y\in Y, s\in S, t\in T\setminus\{1,...,DM_g\} \tag{A.2g}$$

The variable x_{ig}^{y} in Eq. (A.2a) keeps track of the cumulative investment decisions made for each new generator belonging to the set $G^{(new)}$, at each node i over the years y up to the

end of the planning horizon. The maximum annual budget for investment in new generators within a specific region belonging to the set I^c (e.g. a specific region or country) is limited in Eq (A.2b). Similarly, Eq (A.2c) ensures that the adequacy reserve margin for conventional (dispatchable) generation units is respected for a specific region or system. Eq (A.2d) ensures the coupling between investment and operational decisions, indicating that only existing units may be committed for operation and power dispatch. Eq (A.2e) defines the hourly unit commitment state of the generation units through the start-up and shut-down decisions. Finally, Eq. (A.2f) and Eq. (A.2g) constraint the minimum allowable up- and down-times for thermal and nuclear units.

Power dispatch constraints

$$\sum_{g\in G} p_{ig}^{yst} + lns_i^{yst} - \sum_{j\in N_{(i)}^+} f_{ij}^{yst} + \sum_{j\in N_{(i)}^-} f_{ji} = L_i^{yst}, \forall i \in I, y \in Y, s \in S, t \in T \tag{A.3a}$$

$$\sum_{s\in S}\sum_{t\in T}\sum_{g\in G^{(res)}} p_{ig}^{yst} \geq Res^{(lvl)} \cdot \sum_{s\in S}\sum_{t\in T} \bar{L}_i^{yst}, \forall i \in I^c, y \in Y \tag{A.3b}$$

$$p_{ig}^{yst} \leq u_{ig}^{yst} \cdot \bar{P}_g, \quad \forall i \in I, g \in G^{(th)}, \forall y \in Y, s \in S, t \in T \tag{A.3c}$$

$$p_{ig}^{yst} \geq u_{ig}^{yst} \cdot \underline{P}_g, \quad \forall i \in I, g \in G^{(th)}, y \in Y, s \in S, t \in T \tag{A.3d}$$

$$p_{ig}^{yst} - p_{ig}^{yst-1} \leq u_{ig}^{yst-1} \cdot \bar{UR}_g + z_{ig}^{yst} \cdot St\_P_g, \quad \forall i \in I, g \in G^{(th)}, \; y \in Y, s \in S, t \in T \setminus \{1\} \tag{A.3e}$$

$$p_{ig}^{yst-1} - p_{ig}^{yst} \leq u_{ig}^{yst-1} \cdot \bar{DR}_g, \quad \forall i \in I, g \in G^{(th)}, y \in Y, s \in S, t \in T \setminus \{1\} \tag{A.3f}$$

$$p_{ig}^{yst} \leq x_{ig}^{y} \cdot \bar{P}_g \cdot CF_{ig}^{yst}, \quad \forall i \in I, g \in G^{(res)}, \forall y \in Y, s \in S, t \in T \tag{A.3g}$$

$$-2\bar{\theta} \leq \theta_i^{yst} - \theta_j^{yst} - \mathcal{X}_{ij} \cdot f_{ij}^{yst} \leq 2\bar{\theta}, \quad \forall (i,j) \in \mathcal{F}, y \in Y, s \in S, t \in T \tag{A.3h}$$

$$-\bar{f}_{ij} \leq f_{ij}^{yst} \leq \bar{f}_{ij}, \quad \forall (i,j) \in \mathcal{F}, y \in Y, s \in S, t \in T \tag{A.3i}$$

$$-\bar{\theta} \leq \theta_i^{yst} \leq \bar{\theta}, \quad \forall i \in I, y \in Y, s \in S, t \in T \tag{A.3j}$$

$$\theta_i^{yst} = 0, \quad \forall i = i^{ref}, y \in Y, s \in S, t \in T \tag{A.3k}$$

Regarding power dispatch, the hourly supply and demand balance is ensured by Eq. (A.3a). In this constraint, the total power generated, the total load-not-supplied and the total power flow from and to each node, is equal to the power demand at this node. Eq (A.3b) ensures a minimum of IRES production required in the system, according to the particular policy of the decision maker, based on a maximum estimate for the forecasted demand time-series. The hourly maximum and minimum production levels for thermal and nuclear units, once committed, are given in Eq (A.3c) and Eq. (A.3d), respectively. Eq. (A.3e) and Eq. (A.3f) limits the hourly upwards and downwards ramping capabilities for thermal and nuclear units, respectively, to their maximal technical capabilities. If the generation unit is starting-up, its ramping upwards is also constrained by the maximum start-up generation level, as seen in Eq. (A.3e). IRES generation at each node is limited by the hourly available capacity factor $\boldsymbol{CF}$, which is related to wind speeds and solar irradiance, as described in Eq (A.3g).

Bi-directional power flow between network nodes is described by constraints (A.3h)-(A.3k). Eq. (A.3h) sets the power flow magnitude and direction between nodes based on the difference in voltage angles and the susceptance of the transmission line. The maximum flow in each transmission line is limited by constraint (A.3i) in both power flow directions. Similarly, the voltage angle is constraints within the physical limits set in Eq. (A.3j). Finally, the voltage angle for the selected reference node is set to zero, as indicated by constraint (A.3k).